Fatigue Assessment of Full-Scale Retrofitted Orthotropic Bridge Decks

Teixeira De Freitas, Sofia; Kolstein, Henk; Bijlaard, Frans

DOI
10.1061/(ASCE)BE.1943-5592.0001115

Publication date
2017

Document Version
Accepted author manuscript

Published in
Journal of Bridge Engineering

Citation (APA)
Teixeira De Freitas, S., Kolstein, H., & Bijlaard, F. (2017). Fatigue Assessment of Full-Scale Retrofitted Orthotropic Bridge Decks. *Journal of Bridge Engineering*, *22*(11), Article 4017092. https://doi.org/10.1061/(ASCE)BE.1943-5592.0001115

FATIGUE ASSESSMENT OF FULL-SCALE RETROFITTED ORTHOTROPIC BRIDGE DECKS

Sofia Teixeira de Freitas[1)], Henk Kolstein[2)], and Frans Bijlaard[3)]

1) Assistant Professor, Faculty of Aerospace Engineering, Delft University of Technology, S.TeixeiradeFreitas@tudelft.nl
2) Associate Professor, Faculty of Civil Engineering and Geosciences, Delft University of Technology, M.H.Kolstein@tudelft.nl
3) Full Professor, Faculty of Civil Engineering and Geosciences, Delft University of Technology, F.S.K.Bijlaard@tudelft.nl

Abstract: Full-scale fatigue tests were performed on two retrofitted orthotropic bridge decks (OBD). The retrofitting systems consist of adding a second steel plate on the top of the existing deck. The aim is to reduce the stresses at the fatigue sensitive details and therefore extend the fatigue life of the OBD by stiffening the existing deck plate. Two retrofitting systems have been studied. The bonded system consists in bonding a second steel plate to the existing deck by vacuum infusing a thin adhesive layer (2 mm) between the two steel plates. The sandwich system consists in bonding the second steel plate through a thick polyurethane core (15 mm). The aim of the study was to assess the fatigue performance of both retrofitting. No fatigue damage was detected in the retrofitting layers during fatigue tests after 3 million cycles of wheel load. The stresses close to the deck-plate-to-stiffener welds reduce by at least 55% when using the bonded steel plates system and 45% when using the sandwich steel plates system. Both systems proved to have sufficient fatigue life to withstand traffic wheel loads running on orthotropic bridge decks and help extending the fatigue life of the existing OBD.

Key Words: *Orthotropic steel bridge decks, Reinforcement, Fatigue, Structural bonding, Sandwich structures*

INTRODUCTION

Orthotropic steel bridge decks (OBDs) are largely used in most of the major long span bridges in the world due to their low dead-weight at an attractive cost. However, in the past decades, severe fatigue cracks have been reported at several welded joints in OBDs (Jong 2004, Fisher 2016). One of the most threatening is the one that grows through the deck plate at the longitudinal welds between the deck plate and trapezoidal stiffener (deck-plate-to-stiffener weld) (Ya et al 2011). These welds have very high stress concentrations particularly at the intersection with the crossbeams (Kolstein, Wardenier, and Weijde

1998). The major reason for these fatigue cracks is the low stiffness of the deck plate, which is insufficient to deal with the heavy traffic wheel loads (Miki 2006). Moreover, the increase of heavy traffic in the past decades makes these fatigue phenomena an even greater concern.

Several research projects studied different renovation systems to strengthen existing OBDs. The common idea is to substitute the existing asphalt wearing course by a stiffer overlay. Research has been done on replacing the wearing course by a reinforced concrete overlay (Walter 2005, Jong 2006, Zhang et al 2016). Field measurements performed during renovations of several orthotropic brides in the Netherlands, where the common 50 mm thick asphalt surface was replaced by 50 mm thick reinforced concrete overlay, showed a stress reduction close to the welds of 80% after the reinforcement when compared with no surfacing (Kolstein and Sliedrecht 2008). Alternative wearing courses solutions to the classic asphalt layer have been also proposed by Medani (2006). Other retrofitting techniques focus on delaying the crack propagation by acting directly at the welded areas, such as Impact Crack-closure Retrofit (ICT), by inducing compressive residual stresses introduced by plastic deformation through high-speed impact (Yamada et al 2015, Zhiyuan et al 2016).

However, most of the mentioned alternatives for replacing the existing wearing course are often too heavy for application on existing movable bridges with orthotropic decks. For these structures, the weight limits are very strict and light-weight retrofitting overlays are the only possible solution. Previous studies have suggested light weight retrofitting systems which consist of adding a second steel plate to the existing deck. The second (new) steel plate is bonded to the existing deck either by vacuum infusing a 2 mm thick adhesive layer between the two steel plates (Labordus 2006) – referred in this paper as bonded steel plate system, or by a 15 to 30 mm thick polyurethane core – referred in this paper as sandwich steel plate system (Vincent and Ferro 2004). Both retrofitting solutions are regarded as lightweight - between 50 and 80 kg/m^2. Previous research

performed on beams representing the mentioned retrofitting overlay systems show stress reduction factors between 60% and 75% at the existing deck plate after retrofitting (Teixeira de Freitas et al., 2010, 2011, 2013a). Structural monitoring of a pilot application of the bonded system with 6 mm thick second steel plate retrofitting a 12 mm thick exiting deck plate of the Scharsterrijn movable bridge in the Netherlands showed 55% stress reduction at the deck-plate-to-stiffener weld after renovation (Teixeira de Freitas et al 2012a). Further application of the same system in Hartelkanaal 12 mm thick existing deck plate with 10 mm thick second steel plate promised an additional fatigue service life to the existing deck of 40 years (Voermans et al 2014). A trial full-scale application of the sandwich steel plate system also showed significant reduction in the deck deflection and the additional advantages in terms of thermal insulation and decreased noise emission (Feldmann et. al 2007). Full scale static tests of the steel-polyurethane OBD showed stress reduction from 40% to 80% close to the fatigue-sensitive details and a good performance under compressive longitudinal stresses (Teixeira de Freitas et al 2013b, Shan C. and Yi Y. 2016, 2017, Shan C 2017). Nevertheless, the retrofitting systems also have to be evaluated in terms of fatigue performance. When applying a reinforcement system to a fatigue cracked OBD, it is important to guarantee that the reinforcement system will not raise new fatigue problems to the structure.

In this paper, full scale fatigue test are performed on OBD reinforced with bonded steel plate system and sandwich plate system in order to evaluate and compare their fatigue performance under full-scale. The aim is to determine the fatigue life of both retrofitting systems when subject to realistic wheel loads.

BRIDGE DECK SPECIMENS

Two orthotropic deck-panels were manufactured with the same geometry: one was retrofitted using the bonded system and another using the sandwich system.

Figure 1 shows a drawing of the deck specimens. The specimens were 5000 mm long and 2000 mm wide. The deck plate was 12 mm thick and it was reinforced by three longitudinal trapezoidal stiffeners (Krupp profile FHK 2/325/6: height of 325 mm, a base distance between the outer side of the trough legs of 300 mm, bottom width of 105 mm and a plate thickness of 6 mm) and two transverse crossbeams 3000 mm apart. In a real bridge, the traffic runs in the longitudinal direction on top of the deck plate. The deck is made of steel grade S355 (f_y = 355 MPa, f_u = 510 MPa, E = 210 GPa, υ = 0.3) (EN 1993-1-1 2006).

Figure 2 shows the nominal thicknesses of the bonded and sandwich retrofitting systems. In the bonded system, a 6 mm thick second steel plate was bonded to the existing 12 mm thick deck plate with a 2 mm thick adhesive. In the sandwich system, a 5 mm thick second steel plate was bonded to the 12 mm thick existing deck plate with a 15 mm thick polyurethane core.

The second steel plate is made of steel grade S355. The adhesive is an epoxy paste resin - Epikote resin EPR 04908 with hardener Epikure curing agent EPH 04908 (properties at room temperature: E_t = 2929 MPa; σ_{tmax} = 69 MPa; υ = 0.4 (Teixeira de Freitas, Kolstein and Bijlaard 2010)). The core material is a polyurethane with density 1150 kg/m^3 (properties at room temperature: E_t = 721 MPa; σ_{tmax} = 25 MPa; υ = 0.36 (Teixeira de Freitas, Kolstein and Bijlaard 2011)).

The manufacturing procedure of the bonded system consisted on the following chorological steps: (1) grit blast and clean the steel surfaces (Sa 2 1/2 - ISO 8501 (2007)); (2) apply a primer on the steel surfaces to be bonded; (3) glue spacers with thickness of 2 mm; (4) place the new steel plate on the top of the existing deck; (5) prepare the cavity between the steel plates for infusion; (6) vacuum infuse the adhesive and (7) cure during 16 hours between 40˚C and 50˚C.

The manufacturing procedure of the sandwich system consisted on the following chronological steps: (1) grit blast and clean the steel surfaces (Sa 2 1/2 - ISO 8501 (2007)); (2) weld steel bars with the core thickness on the perimeter of the existing deck plate; (3) glue PU spacers with the core thickness; (4) place the new steel plate on the top of the perimeter bars and weld

through the perimeter; (5) inject the PU into the cavity between the steel plates and (6) cure at room temperature during 48 h.

Instrumentation

Strain gauges were glued to the bottom side of the deck, at three cross-sections: two crossbeams (A and B) and midspan between both crossbeams - see Figure 1. The location of the strain gauges is shown in Figure 3.

The position of the strain gauges was the same for both deck specimens. In order to apply the strain gauges inside the troughs, parts of the troughs were cut out and re-welded again.

The strain gauges were positioned to measure transverse strains, except the ones at the bottom of the stiffeners at the midspan, which measure longitudinal strains. The exact location of the strain gauges close to the deck-plate-to-stiffener welds is shown in Figure 4.

EXPERIMENTAL PROCEDURE

The deck specimens were loaded with wheel prints type C at the crossbeam cross-sections and at midspan between crossbeams, in accordance with the fatigue load models of EN 1991-2 (2003). Wheel print type C is a single-tyre 320 mm long and 270 mm wide, usually called super-single.

In total seven fatigue test were performed on each deck specimen. At the crossbeams, six fatigue tests were performed in total, one on each trough-to-crossbeam joint (2 crossbeams x 3 troughs). Wheel type C was aligned with the crossbeam's web and with each trough. Figure 5 shows one example of a fatigue test performed at the crossbeam A (trough 2-to-crossbeam A joint). At midspan between crossbeams, one fatigue test was performed with wheel type C aligned with the middle trough. The seven fatigue tests on each deck specimen were performed one by one. The same load cases were used for both deck specimens. Prior to the fatigue tests, static tests were performed with the same wheel print and location as the fatigue tests.

110 The bottom flanges of the two crossbeams were clamped to the ground. Figure 6 shows a photo of the test set up. The
111 load was applied on the deck through a 30 mm thick steel plate and 30 mm thick rubber plate, with the rectangular area of the
112 wheel print type C.

113 The fatigue tests were carried out under load control with a constant applied load ratio R = 0.1 ($R = P_{min} / P_{max}$). The wave
114 form was sinusoidal. The bonded steel plates specimen was loaded at a frequency of 7 and 5 Hz at the crossbeam
115 cross-sections and at midspan between crossbeams, respectively. The sandwich steel plates specimen was loaded at a
116 frequency of 2 Hz at both locations. Previous research on sandwich beam specimens has shown that for higher frequencies
117 than 2 Hz, the temperature of the PU core increases with fatigue cycling (Teixeira de Freitas, Kolstein and Bijlaard 2013a). In
118 order to avoid this undesirable thermal effect, the frequency was kept to 2 Hz on the sandwich specimens.

119 The tests were performed at three load levels. The maximum loads P_{max} were 160 kN, 110 kN and 90 kN (ΔP= 144 kN,
120 99 kN and 81 kN, respectively). At the crossbeams, two tests were performed at each load level. At midspan between
121 crossbeams, the bonded steel plates specimen was tested at P_{max} = 160 kN and the sandwich steel plates at P_{max} = 110 kN.
122 Chronologically, the bonded steel plates specimen was tested first, and when tested at midspan between crossbeams, a fatigue
123 crack appeared in an early stage at the weld of the trough made for the instrumentation holes. The test had to be stopped, the
124 trough was cut out and replaced by larger piece in order to reduce the stresses at the welds. After re-welding the new
125 trough-piece, the test was restarted. In order to avoid this problem on the sandwich steel plates specimen, the maximum load
126 level at midspan between crossbeams was decreased to 110 kN. No fatigue crack was detected at the trough of this specimen.

127 The load levels used in the fatigue tests are higher than the ones recommended at the fatigue load model 2 of EN1991-2
128 (2003). In the fatigue model, the maximum load of wheel type C is 60 kN. The loads used in the fatigue tests are from 1.5 to

129 2.67 times higher than the ones described by the fatigue model.

130 Ultrasonic Non-Destructive-Testing A-scan was performed at the loaded areas of the bonded steel plates reinforced
131 specimen. The aim was to detected delamination areas of the adhesive layer. The scanning was performed before and after the
132 fatigue tests, and every million cycles.

133 **FINITE ELEMENT ANALYSIS**

134 A Finite Element Analysis was performed to determine the stress fields in the OBD during testing. The geometry, wheel
135 loads and boundary conditions of the model were simulating the full-scale test. The commercial FEA program ABAQUS was
136 used to run the simulations.

137 The geometry of the model follows the nominal dimension of the several parts of the OBD. The welds were modeled
138 only as the geometrical connection between the deck plate, stiffeners and cross beams. The linear elastic mechanical properties
139 of the materials mentioned previously were used. Figure 7 shows a 3D view of the model. Only half of the deck plate has
140 been model and a symmetry boundary condition was applied at midspan. More details on the numerical work, including mesh
141 details, element type, number of nodes and mesh convergency study can be found in Teixeira de Freitas (2012b, 2013b).

142 **RESULTS**

143 **Static tests and numerical validation**

144 In order to validate the numerical results, the strains measured by the strain gauges during the static tests are compared
145 with the strains from the FEM. Figure 8 shows the transverse strain values measured during a static test with 100 kN wheel
146 type C positioned at the cross beam location, both for the bonded system and the sandwich system. The transverse strains on
147 the bottom side of the deck plate measured by the strain gauges at the crossbeam and at 75 mm from the crossbeam are

compared with the numerical strains from the FEM at the same locations. Figure 9 shows the results of a static test of 100 kN wheel type C positioned midspan between crossbeams. Also here, the strain measured by the strain gauges are compared with the numerical strains.

For both reinforcement systems, the strains measured close to the deck-plate-to-stiffener welds are higher at the cross beam location than at midspan. This stress concentration is caused by the stiffness singularity introduced by the cross beam web. Also important to notice is that, at the cross beam location, the non-loaded troughs experience an insignificant strain when the adjacent trough is loaded. This shows that the fatigue test results at the crossbeam location at the three different troughs can be treated as separate tests.

For both reinforcement systems and load locations, the numerical results correspond well with the experimental results.

Fatigue tests

Figure 10 shows a selection of strain ranges versus the number of cycles, measured on the bonded steel plates reinforced deck. Figure 10a shows the results of eight strain gauges close to a deck-plate-to-stiffener weld in one of the crossbeam fatigue tests. The maximum load in this example was 160 kN. Strain gauge SG05, SG06 and SG 07 are close to the weld root, SG01 and SG03 are close to the weld toe and SG09, SG10 and SG11 are between stiffeners webs. From all gauges at this location, the one with the biggest change during testing is strain gauge SG06. This strain gauge is aligned with the crossbeam web, close to the weld root. The range started to decrease in an early stage of the fatigue tests. As a response to that decrease, strain range SG01 and SG03 started to increase. This is a consequence of the stress redistribution due to the local stiffness loss close to strain gauge SG06. The fatigue tests at lower load levels showed a similar strain pattern but at lower magnitudes. Figure 10b shows the strain ranges measured during the fatigue test at midspan on the deck reinforced with the bonded system. Strain

gauge SG8 and SG9 are close to the deck-plate-to-stiffener weld root, SG3 and SG4 are close to the weld toe, and SG12 and SG13 are between stiffeners' webs. The maximum load level was P_{max} = 160 kN. There were no significant changes during testing in any of the strain gauges results. The main difference between the tests at the crossbeam (Figure 10a) and at midspan (Figure10b) is the strain close to the welds, which are significantly lower at midspan than at crossbeam location (at midspan SG9 is less than 100μ, while at the crossbeam SG06 is approximately 500μ). The crossbeam's web is a point of very high stiffness which leads to high stress concentration. The strain between the stiffener webs is higher at midspan between crossbeams than at the crossbeam (SG13 is approximately 900μ at midspan, while SG10 is 600μ at the crossbeam).

The ultrasonic NDT performed before and after the fatigue tests didn't detect any change in the integrity of the adhesive layer in none of the locations. This means that there was no delamination in the adhesive layer caused by the fatigue loading.

Figure 11 shows the strain ranges measured on the sandwich steel plates reinforced deck for the same selection of strain gauges. In general, the strain ranges measured at the sandwich steel plates deck specimen have a very similar pattern to the corresponding ones measured at the bonded steel plate deck specimen. In Figure 11a, the biggest change in the strain range occurs at the same deck location, strain gauge SG06. The range also started to decrease in an early stage of the fatigue tests. The major difference between the bonded and sandwich reinforced decks is the strain magnitude of SG06 at the maximum load level (P_{max}=160 kN). In the bonded reinforced deck the initial strain range is approximately 550μ while in the sandwich reinforced deck the initial strain range is approximately 725μ. Figure 11b shows the strain ranges measured during the fatigue test at midspan on the deck reinforced with the sandwich system. The maximum load was P_{max}=110 kN. There were no significant changes during testing in any of the strains measured. As for the bonded reinforced deck, the strains measured close to the welds are considerably higher at the crossbeam location than at midspan for the same load.

186 The ultrasonic A-scan was not performed on the sandwich steel plates deck specimen, since after a trial test on a reference
187 sandwich panel, it was concluded that the damping of the sound wave when crossing the interface between the steel plate and
188 the PU core material was as high as when crossing an interface between steel plate and air. Therefore, no distinction could be
189 made between good and bad adhesion quality at the interface between the steel and the core.

190 As no major failure was detected in any of the fatigue tests, all tests were stopped after approximately 3 million cycles.

191 During and after the fatigue tests, both bridge deck specimens were visually inspected for fatigue cracks at the welds. At
192 the crossbeam location, several fatigue cracks were observed at the deck-plate-to-stiffener welds. Figure 12 shows pictures of
193 the fatigue cracks close to those welds on both reinforced deck-panels. These pictures were taken after cutting a part of the deck
194 specimens at the crossbeam. At midspan no cracks were observed.

195 The strain gauges showing major changes are always close to the deck-plate-to-stiffener welds, exactly where fatigue
196 cracks were observed. No delamination was detected in the adhesive layer by the ultrasonic NDT. Therefore, it can be
197 concluded that the decrease of strain range close to the welds is caused by fatigue crack initiation at the deck-plate-to-stiffener
198 weld, and not by fatigue damage of the reinforcements. Although at the sandwich steel plates deck specimen, there was no
199 NDT inspection to the interface between the core and the steel plate, the fact that the corresponding strain range pattern is very
200 similar to the bonded steel plates deck panel and that fatigue cracks were also observed at the deck-plate-to-stiffener welds, it
201 can be concluded that: there was no fatigue damage on the sandwich steel plates reinforcement.

202 It is important to remember that the main objective of the full-scale fatigue tests was to evaluate the fatigue behavior of the
203 retrofitting systems, rather than the fatigue life of the welds on an OBD. As no delamination was detected in the adhesive layer
204 in none of the fatigue tests, it can be considered that the seven fatigue tests on the bonded steel plates retrofitted deck were run

205 out test (no fatigue failure). The same can be said for the sandwich steel plate retrofitted deck as there was no indication of
206 delamination in the sandwich overlay in none of the seven fatigue tests.

207 Table 1 summarizes the fatigue results of the deck-plate-to-trough weld on both retrofitted deck specimens. The fatigue
208 life n_f is based on the strain ranges measured by the gauges close to the deck-plate-to-stiffener weld roots, aligned with the
209 crossbeam or with midspan between crossbeams (SG06 at the crossbeam and SG09 at midspan). The results are presented for
210 two different failure criteria: 10% and 25% strain fall. These failure criteria were used by (Kolstein 2007) to define the fatigue
211 design classification of this type of fatigue crack (cracks at deck-plate-to-stiffener weld that grow through the deck-plate
212 thickness). The main difference is that (Kolstein 2007) used strain gauges on the top side of the deck plate and, in this study,
213 strain gauges on the bottom side of the deck-plate were used. At each fatigue test, two deck-plate-to-stiffener welds were tested
214 simultaneously and, therefore, the fatigue results are presented for both welds (one at each side of the stiffener). When no
215 changes were observed in the measured strain ranges during fatigue tests and no cracks were detected, the tests were
216 considered run-out tests.

217 **DISCUSSION**

218 In this section, the results of the full-scale fatigue tests are discussed mainly to evaluate the fatigue life of the retrofitting
219 systems. The results are compared with SN curves proposed in previous research. In order to make this comparison, it is
220 important to know the stress distribution in the retrofitting layers during the full-scale testing. This distribution was determined
221 by Finite Element Analysis (FEA) of the full-scale tests already presented.

222 Since several fatigue cracks were found during fatigue testing, a brief analysis of the fatigue life of the welded joints of the
223 retrofitted deck is presented in the end of this section.

224 **Stress distribution in the retrofitting systems**

225 Previous research in beam specimens showed that the main fatigue failure mode of the bonded steel plates system when
226 subject to four-point bending tests (bending and shear location) is adhesive shear failure (Teixeira de Freitas, Kolstein and
227 Bijlaard 2013a). For the same tests performed in the sandwich steel plates system, the main fatigue failure observed was
228 delamination between the steel face and the core. Therefore, the fatigue behavior of the bonded and sandwich retrofitting
229 systems depends on the shear stress in the adhesive layer and at the interface between the steel face and the core, respectively.

230 The shear stress distribution in the reinforcement systems during the full scale test was determined by the FEA. Figure 13
231 shows one example of the shear stress distribution τ_{xy} along the width of the deck in the adhesive layer (Figure 13a) and in the
232 interface between the steel plate and the core (Figure 13b). τ_{zy} was neglected since the values were significantly lower than τ_{xy}.
233 Two load cases are presented: wheel type C at midspan between crossbeams and wheel type C at the crossbeam cross section.
234 On both cases the wheel is aligned with the middle trough.

235 The maximum shear stress in the adhesive layer of the bonded steel plates system occurs at x=900 mm and x=1100 mm,
236 in between the stiffeners webs (Figure 13a). For 100 kN wheel load, the maximum shear stress is approximately 8 MPa at the
237 crossbeam cross section and 7 MPa at midspan between crossbeams. Figure 13b shows the results of the shear stress at the
238 steel-plate-core interface of the sandwich steel plates system. The maximum values between the two interfaces with the steel
239 plates were taken. The maximum shear stress also occurs at x=900 mm and x=1100 mm. For 100 kN wheel load, the
240 maximum shear stress is approximately 2.3 MPa at the crossbeam cross section and 2.1 MPa at midspan between crossbeams.

241 **Fatigue behavior of the retrofitting systems**

242 The end of the fatigue life of the bonded steel plates system should be taken at the moment when delamination occurs in

243 the adhesive layer. As no delamination was detected after any of the full-scale fatigue tests, it is concluded that no fatigue
244 damage occurred on the bonded steel plates system during full-scale fatigue testing. The same can be considered for the
245 sandwich steel plates system as no delamination was detected during any of the full-scale fatigue tests.

246 Figure 14 shows the stress-cycle SN diagrams for both reinforcements. In Figure 14a, the fatigue life n_f of each fatigue test
247 performed in the bonded steel plates retrofitted deck, is plotted against the shear stress range at the adhesive layer $\Delta\tau_{ad}$. The
248 shear stress range is the maximum shear stress, presented in Figure 13a, multiplied by the amplitude load in the correspondent
249 fatigue test ($\Delta P = 0.9 \cdot P_{max}$). Figure 14b plots the fatigue life n_f of each fatigue test, performed in the sandwich steel plates
250 retrofitted deck, against the shear stress range at the interface between core and steel plate $\Delta\tau_c$. The shear stress range is the
251 maximum shear stress, presented in Figure 13b, multiplied by the amplitude load in the correspondent fatigue test. The results
252 from the full-scale tests are plotted together with fatigue results obtained in previous research from four-point bending fatigue
253 tests on both retrofitting systems (Teixeira de Freitas, Kolstein and Bijlaard 2013a).

254 For the bonded steel plates system, the shear stress at the full-scale tests is close to the fatigue threshold of the adhesive
255 layer proposed in Teixeira de Freitas (2013a), approximately 8 MPa. For the sandwich steel plates system, the shear stress at
256 the interface on the full-scale tests is lower than the fatigue threshold proposed in Teixeira de Freitas (2013a), approximately 4
257 MPa. Therefore, the results from the full-scale fatigue tests are in agreement with the SN curves of both reinforcement systems
258 proposed by Teixeira de Freitas (2013a).

259 **Fatigue life of the welded joints of the retrofitted deck**

260 Although it was not the main objective of the full-scale test, a brief analysis of the fatigue life of the welded joints of the
261 retrofitted bridge decks is presented in this section since several fatigue cracks were found during fatigue testing.

As shown in Figure 12, the crack found at the crossbeam location is the well-known fatigue crack at the deck-plate-to-stiffener weld. The crack starts at the root of the weld between the longitudinal stiffener and the deck plate, at the point where it intersects with crossbeam web. The crack grows through the thickness of the deck plate, from the bottom to the top side of the plate (Kolstein 2007).

Figure 15 shows the SN results of the welds at the crossbeam location, based on both criteria described in Table 2. The stress range $\Delta\sigma$ is determined at the point where the crack initiates, which means at the deck-plate-to-stiffener weld root on the bottom side of the deck plate. For this typical detail, as the stress gradient close to the weld is very high, the stress is determined based on the geometrical stress range - hot spot method. The hot spot method is recommended by Hobbacher (2009), for fatigue assessment of general welded joints and, by Kolstein (2007) for this specific fatigue crack of orthotropic steel bridge decks. The method consists in extrapolating the structural stress from two measuring points to where the crack initiates, called hot spot point. The two measuring points are $0.4t$ and t from the hot spot point, t being the deck plate thickness (12 mm). The stress at the measuring points were taken from the FEA of the full-scale tests. The fatigue life of the welds is compared with the fatigue strength SN curve defined at EN1993-1-9 (2005). The detail category 125 is the one recommended by Kolstein (2007) for these types of fatigue cracks.

The fatigue results of the welds in the bonded and sandwich retrofitted decks follow the same tendency when considering the same criteria for the fatigue life. The fatigue life of the welds in the sandwich retrofitted deck is slightly longer than in the bonded retrofitted deck. The slope of the fatigue results is closer to the fatigue strength of the 125 detail category when the 25% strain fall failure criterion is used. However, the results are worse than expected, since the detail category 125 should give conservative fatigue strength of the fatigue life of these welds. This is related with the fact that, in this study the failure criteria

are based on strain falls measured at the bottom side of the deck plate, very close to the weld root. Kolstein (2007) based his recommendation on strain falls measured at the top side of the deck plate, and therefore farther away from the weld root. As this type of crack initiates at the weld root, the strain measured in this study are much more sensitive to the crack initiating at the weld root than the ones used by Kolstein (2007). Therefore the strain fall occurs earlier in the strain gauges used in this study (at the bottom side of the deck plate) than in the ones used by Kolstein (2007) (at the top side of the deck plate).

From extrapolation of these SN curves, one can predict the fatigue life of the welds at any stress range present at the weld root, in a bonded or sandwich steel plates retrofitted deck. This means that, if one can determine the stress reduction at the weld root after the retrofitting, one can predict the improvement in the fatigue life of the weld just by using the stress reduction factors on these SN curves.

Figure 16 shows the SN results of the welds at midspan between crossbeams. As no fatigue cracks were found, all results are run-out tests. The stress range was determined by the nominal stresses at the deck plate at the stiffener web location. The results are compared with the details category for the fatigue strength of these welds recommended by Kolstein (2007) (125 detail category) and by at EN1993-1-9 (2005) (71 detail category). The results are below the constant amplitude fatigue limit ($\Delta\sigma$ at 5 million cycles) of the 125 detail category, which explains the absence of fatigue cracks at this location.

INFLUENCE OF THE RETROFITTING THICKNESS – PARAMETRIC STUDY

Based on the previous analysis, one can conclude that the fatigue assessment of a retrofitting system for OBD can be performed by:

(1) Determine the Stress Reduction Factor (SRF) at the critical welded joints of the bridge deck;

(2) Determine the fatigue threshold of the retrofitting system.

300 The first one will allow to predict the increase of the fatigue life span of the OBD, and the second one will guarantee that the
301 retrofitting system has a longer fatigue life than the bridge deck. In this section this analysis will be performed to different
302 thickness of the bonded and sandwich steel plates retrofitting system from the ones tested in the full-scale bridge decks.
303 Therefore the influence of the thickness on the efficiency of the retrofitting system will be analyzed. The FEA mentioned
304 earlier in this paper will be used to simulated the different retrofitting scenarios. The load condition simulated was 100kN
305 wheel type C aligned with the middle trough and positioned either at the crossbeam (see Figure 5) or at midspan between
306 crossbeams.
307 Table 2 shows the different retrofitting system simulated. For the bonded steel plates system, the adhesive thickness was kept 2
308 mm, since this is the nominal value to be applied in actual retrofitting, and the thickness of the second steel plate was varied
309 between 6 mm and 12 mm. For the sandwich steel plates systems, the thickness of the core was varied between 15 mm and 30
310 mm, and the thickness of the second steel plate was varied between 5 mm and 8 mm. The retrofitting weight is also shown as a
311 comparative parameter between the different solutions. For all cases studied, the thickness of the existing deck plate is 12 mm.
312 **Stress reduction factor**
313 The SRF was determined using equation (1). The SRF was determined at four deck locations -- see Figure 17. The values were
314 determined at the crossbeam location and at midspan between crossbeams.
315 $$SRF = 1 - \frac{\sigma_{retrofitted\ deck}}{\sigma_{un-retrofitted\ deck}} \quad (1)$$
316 Figure 18 and 19 show the SRF as a function of the weight for the bonded and sandwich steel plates system, respectively. SRFs
317 higher than 100% occur when the stress value changes the signal from negative to positive, or the other way around. The SRF
318 of details I, II and III gives an indication of the retroffiting performance at the transverse stresses due to local bending of the

deck plate.

For the bonded steel plates system B.12.2.6 tested in the full-scale bridge decks, the transverse stresses close to the deck-plate-to-stiffener welds (group II and III) reduce approximately 55% to 60% at the cross beam location after the retrofitting, and about 70% to 90% at the midspan between crossbeams. At the same locations, the sandwich steel plates system S.12.15.5, the stresses reduce approximately 45% at the crossbeam location and 50% to 60% at the midspan between crossbeams. The least affected stresses are the longitudinal stresses at the bottom of the stiffeners (Group IV). The stress are reduced by 20% in the B.12.2.6 solutions and by 30% in the S.12.15.5 solutions.

Concerning details I, II and III both at the crossbeam and at midspan between the crossbeam, the results show that: increasing the thickness of the second steel plate of the bonded steel plates reinforcement by 2 mm adds on average 6% to the SRFs; each increase of 5 mm of core thickness of the sandwich steel plates adds on average 3% to the SRFs. Increasing the thickness of the second steel plate of the sandwich steel plates from 5 mm to 8 mm adds 7% to the SRFs.

Comparing the two retrofitting systems with the same weight, for details I, II and III at the crossbeam location, the SRFs are higher when using the bonded steel plates than when using the sandwich steel plates. The sandwich steel plates system can achieve SRF similar to the ones of the bonded steel plates system but needs double the weight.

At midspan between crossbeams, the SRF of details II and III increases significantly when compared to the ones at the crossbeam location, especially that of detail III of the bonded steel plates.

Also at midspan between crossbeams when comparing two systems with the same weight, details II and III have higher SRF in the bonded steel plates system than in the sandwich steel plates system. The SRF of detail I are similar in the sandwich steel plates reinforcement and in the bonded steel plates systems.

For detail IV, the sandwich steel plates system performs better than the bonded steel plates system. This detail gives an indication of the global effect of the reinforcement (longitudinal stress due to global bending of the OBD).

Figure 19 (b) shows that the SRF of the solution S.12.15.8 (80 kg/m^2) at midspan between crossbeams is slightly out of the tendency. The overall tendency of the graph gives an idea of the effect of the core thickness, while the S.12.15.8 gives an indication of the effect of the second steel plate thickness. The results indicate that this effect is positive for detail III and negative for details I and IV.

Overall, the bonded steel plates system has a good performance in reinforcing the structure locally, as for example close to the deck-plate-to-stiffener welds. The sandwich steel plates system is more a global reinforcement. It affects not only the local stresses, but also the global stresses. The sandwich steel plates systems improves its performance, when the existing steel deck becomes flexible (less stiff), and the bending of the deck becomes larger. This is the case in detail I and detail IV at midspan between crossbeams.

Fatigue life of the retrofitting system

Besides extending the fatigue life of the welds, the reinforcements should not give rise to new fatigue problems. Therefore it is important to evaluate their fatigue life.

The full-scale fatigue tests showed no fatigue damage in the retrofitting systems. This result could have been predicted based on the SN diagrams of each retrofitting system obtained from the fatigue tests on retrofitted beams – see Figure 14. The maximum shear stresses values in the adhesive layer and in the core during the fatigue full scale tests were in the vicinity or below the fatigue thresholds of those SN diagrams.

Table 3 shows the maximum shear stress τ_{xy} at the adhesive layer and at the steel-core interface obtained from the FEA of the

bonded and sandwich steel plates system, respectively. The values correspond with a 100 kN wheel load type C aligned with the stiffener either at the crossbeam location or at midspan between crossbeams.

The retrofitting solutions tested on the full-scale fatigue tests, B.12.2.6 and S.12.15.5 for the bonded and sandwich respectively, have the highest values of shear stress. Therefore, if no fatigue damage was observed during the fatigue tests performed on those retrofitting solutions, no fatigue damage is expected to occur in all the other reinforcements with lower shear stresses.

CONCLUSIONS

The fatigue life of full-scale retrofitted orthotropic bridge deck specimens was investigated. Two retrofitting solutions were compared which consisted in bonding a second steel plate to the existing deck either using a thin 2 mm thick adhesive layer (bonded system) or a thick 15 mm thick polyurethane core (sandwich system). The retrofitted deck specimens were cyclically loaded by single tire wheel prints at the crossbeam cross section and at midspan between crossbeam. From the analysis of the full-scale tests, the following conclusions can be drawn:

- The fatigue threshold of the retrofitting systems determined on beam tests under bending is valid for the fatigue life of the retrofitting system on full-scale OBD under wheel loads.
- Under maximum wheel loads between 160 kN and 90 kN, the stresses at the retrofitting systems are lower than their fatigue threshold. The retrofitting solutions proved to have sufficient fatigue life to withstand traffic wheel loads running on orthotropic bridge decks, without fatigue damage.
- The fatigue evaluation of a retrofitting system for OBD can be performed by determining the Stress Reduction Factor (SRF) at the critical welded joints of the bridge deck and the fatigue threshold of the retrofitting system.
- Using the bonded system, the transverse stresses close to the deck-plate-to-stiffener weld reduce by at least 55%

at the crossbeam location and 70% at midpsan between crossbeams. Each 2 mm added to the thickness of the second steel plate will reduce the stresses 6% further. Using the sandwich system, the same stresses are reduced by at least 45% at the crossbeam location and 55% at the midspan between crossbeams. Each 5 mm added to the sandwich core thickness will increase the stress 3% further.

- For similar weights, the bonded steel plates system is more efficient in reducing the local stresses close to the welds while the sandwich steel plates system is more efficient in reduction the global stresses of the bridge deck.

ACKNOWLEDGEMENTS

The authors would like to thank Lightweight Structures B.V. and Intelligent Engineering (IE) for applying the reinforcements on the bridge deck specimens. This research was supported by the Dutch Technology Foundation STW (Project No. 05979) and by the Portuguese Science and Technology Foundation FCT (Grant No. SFRH/BD/36264/2007).

REFERENCES

EN 1993-1-1 (2006), *Eurocode 3: Design of steel structures Part1-1: General Rules and rules for buildings*, CEN.

EN 1991-2 (2003), *Eurocode 1: Actions on structures – Part 2: Traffic loads on bridges*, CEN.

EN1993-1-9 (2005). *Eurocode 3: Design of steel structures Part 1-9: Fatigue*, CEN

Feldmann M, Sedlacek G, Geβler A. (2007). "A system of steel-elastomer sandwich plates for strengthening orthotropic bridges decks", *Mechanics of Composite Materials*, 43(2): 183–190.

Fisher, J. and Barsom, J. (2016), "Evaluation of Cracking in the Rib-to-Deck Welds of the Bronx–Whitestone Bridge, *Journal of Bridge Engineering*, 21(3): 04015065.

ISO 8501 (2007), *Preparation of steel substrates before application of paints and related products*, CEN.

Hobbacher, A. (2009). "The new IIW recommendations for fatigue assessment of welded joints and components - A comprehensive code recently updated", *International Journal of Fatigue,* **31** (1), 50 – 58.

Jong de, F. (2004). "Overview fatigue phenomenon in orthotropic bridge decks in the Netherlands", In *2004 Orthotropic Bridge Conference*, Sacramento, USA

Jong de, F. (2006). *Renovation techniques for fatigue cracked orthotropic steel bridge decks*. PhD thesis, Delft University of Technology, Netherlands.

Kolstein, H., Wardenier, J., and Weijde, H. (1998). "A new type of fatigue failures in steel orthotropic bridge decks", In *Fifth Pacific Structural Steel Conference*, Seoul, Korea.

Kolstein, H. (2007). *Fatigue classification of welded joints in orthotropic steel bridge decks*. PhD thesis, Delft University of Technology, Netherlands.

Kolstein, M. and Sliedrecht, H. (2008). "Reduction of traffic induced stresses using high strength concrete". In *2008 International Orthotropic Bridge Conference*, Sacramento, USA.

Labordus M. (2006). "Vacuum infused bonded steel reinforcing plates for bridge rehabilitation." In: *International bridge technology conference and trade show*, Rotterdam, The Netherlands.

Liu, R., Liu, Y., Ji, B. Wang, M. and Tian, Y. (2014), "Hot spot stress analysis on rib–deck welded joint in orthotropic steel decks", *Journal of Constructional Steel Research*, 97, 1-9.

Medani, T. (2006). *Design principles of surfacings on orthotropic steel bridge decks*. PhD thesis, Delft University of Technology, Netherlands.

Miki, C. (2006). "Fatigue damage in orthotropic steel bridge decks and retrofit work", *Steel structures* **6**, 255–267.

Shan C. and Yi Y. (2016). "Stress concentration analysis of an orthotropic sandwich bridge deck under wheel loading", *Journal of Constructional Steel Research*, 122: 488–494

Shan C. and Yi Y. (2017). "An experimental and numerical study on the behavior of a continuous orthotropic bridge deck with sandwich construction", *Thin-Walled Structures*, 111: 138–144

Shan C (2017). "Bending performance of steel–polyurethane sandwich plate under local distributed load", *Advances in Structural Engineering*, 1–8.

Teixeira de Freitas, S., Kolstein, H., Bijlaard, F. (2010), "Composite bonded systems for renovations of orthotropic steel bridge decks", *Composite Structures*, **92**, 853–862.

Teixeira de Freitas, S., Kolstein, H., Bijlaard, F. (2011), "Sandwich system for renovation of orthotropic steel bridge decks", *Journal of Sandwich Structures and Materials*, **13**(3), 279–301.

Teixeira de Freitas, S., Kolstein, H., Bijlaard, F. (2012a), "Structural monitoring of a strengthened orthotropic steel bridge deck using strain data", *Structural Health Monitoring*, **11**(5), 558–376.

Teixeira de Freitas, S (2012b), *Steel plate reinforcement of orthotropic bridge deck*, PhD thesis, Delft University of Technology, Netherlands (uuid:89af64f8-519b-4760-b717-515a3da4e27b).

Teixeira de Freitas, S., Kolstein, H., Bijlaard, F. (2013a), "Fatigue behavior of bonded and sandwich systems for strengthening orthotropic steel bridge decks", *Composite Structures*, **97**, 117–128.

Teixeira de Freitas, S., Kolstein, H., Bijlaard, F. (2013b), "Lightweight reinforcement systems for fatigue-cracked orthotropic bridge decks", *Structural Engineering International*, **4/2013**, 458-467.

Vincent R and Ferro A (2004). " A new orthotropic bridge deck: design, fabrication and construction of the Shenley bridge incorporating a SPS orthotropic bridge deck". In *2004 Orthotropic Bridge Conference*, Sacramento, USA.

Voermans J., Souren W. and Bosselaar M. (2014), "Strengthening the Orthotropic Steel Deck Structure of the Movable Bridge across the Hartelkanaal", *Structural Engineering International*, **3/2014**, 420-424.

Walter, R. (2005). *Cement-based overlay for orthotropic steel bridge decks: a multi-scale modeling approach*. PhD

thesis, Technical University of Denmark, Denmark.

Ya, S., Yamada, K., and Ishikawa, T. (2011), "Fatigue Evaluation of Rib-to-Deck Welded Joints of Orthotropic Steel Bridge Deck", *Journal of Bridge Engineering*, 16(4), 492-499.

Yamada, K., Ishikawa, T. and Kakiichi, T.(2015), "Rehabilitation and improvement of fatigue life of welded joints by ICR treatment", *Advanced Steel Construction*, 11(3), 294-304.

Zhang, S., Shao, X., Cao, J., Cui, J., Hu, J., and Deng, L (2016), "Fatigue Performance of a Lightweight Composite Bridge Deck with Open Ribs", *Journal of Bridge Engineering*, 21(7), 04016039.

Zhiyuan, Y., Bohai, J., Zhongqiu, F. and Hanbin G. (2016) "Fatigue Performance of Cracked Rib-Deck Welded Joint Retrofitted by ICR Technique", *International Journal of Steel Structures* 16(3): 735-742.

Table 1: Maximum load (P_{max}) versus fatigue life (n_f) of the deck-plate-to-stiffener welds ($R = P_{min} / P_{max} = 0.1$).

	Bonded steel plates			Sandwich steel plates		
Location	P_{max} (kN)	n_f (cycles)		P_{max} (kN)	n_f (cycles)	
		10%	25%		10%	25%
Crossbeam	160	72883	112354	160	139565	181320
	160	63225	108994	160	62955	107528
	160	64535	107649	160	52692	79330
	160	48368	72561	160	46573	215155
	110	402821	529840	110	125051	204498
	110	65392	124920	110	274344	369033
	110	107940	189030	110	126719	192044
	110	120544	239029	110	291973	365773
	90	227845	378262	90	125083	228472
	90	98259	203896	90	145685	271185
	90	211682	336889	90	125784	200292
	90	116726	217144	90	>3918743 (run out)	
Midspan	160	>5072367 (run out)		110	>4136051 (run out)	
	160	>5072367 (run out)		110	>4136051 (run out)	

453

454 Table 2 – Retrofitting systems evaluated in the parametric study.

System	Nomenclature	Deck plate	Adhesive or Core[1]	2nd steel plate	Weight
Bonded steel plates	B.12.2.6[2]	12 mm	2 mm	6 mm	49 kg/m^2
	B.12.2.8	12 mm	2 mm	8 mm	65 kg/m^2
	B.12.2.10	12 mm	2 mm	10 mm	81 kg/m^2
	B.12.2.12	12 mm	2 mm	12 mm	97 kg/m^2
Sandwich steel plates	S.12.15.5[2]	12 mm	15 mm	5 mm	57 kg/m^2
	S.12.20.5	12 mm	20 mm	5 mm	62 kg/m^2
	S.12.25.5	12 mm	25 mm	5 mm	68 kg/m^2
	S.12.30.5	12 mm	30 mm	5 mm	74 kg/m^2
	S.12.15.8	12 mm	15 mm	8 mm	80 kg/m^2
	B.12.30.6	12 mm	30 mm	6 mm	82 kg/m^2
	B.12.30.8	12 mm	30 mm	8 mm	97 kg/m^2

455 [1] – *adhesive* when referred to bonded steel plates and *core* when referred to sandwich steel plates

456 [2] –retrofitting solution tested in the full-scale bridge decks

457

458

459 Table 3 – Maximum shear stress τ_{xy} at the adhesive layer and at the steel-core of the bonded and sandwich steel plates system

460 (100 kN load, wheel type C).

τ_{xy} (MPa)	Nomenclature	Adhesive or Interface steel-core[1]	
		Crossbeam location	Midspan between crossbeams
Bonded steel plates	B.12.2.6[2]	7.95	6.95
	B.12.2.8	7.63	6.66
	B.12.2.10	7.14	6.18
	B.12.2.12	6.61	5.64
Sandwich steel plates	S.12.15.5[2]	2.35	2.18
	S.12.20.5	2.23	1.97
	S.12.25.5	2.06	1.92
	S.12.30.5	1.88	1.71
	S.12.15.8	1.74	1.59
	B.12.30.6	1.69	1.55
	B.12.30.8	1.57	1.43

461 [1] – *Adhesive* when referred to bonded steel plates and *Interface steel-core* when referred to sandwich steel plates

462 [2] – retrofitting solution tested in the full-scale bridge decks

463

464

Figure1a

Click here to download Figure fig01a.eps

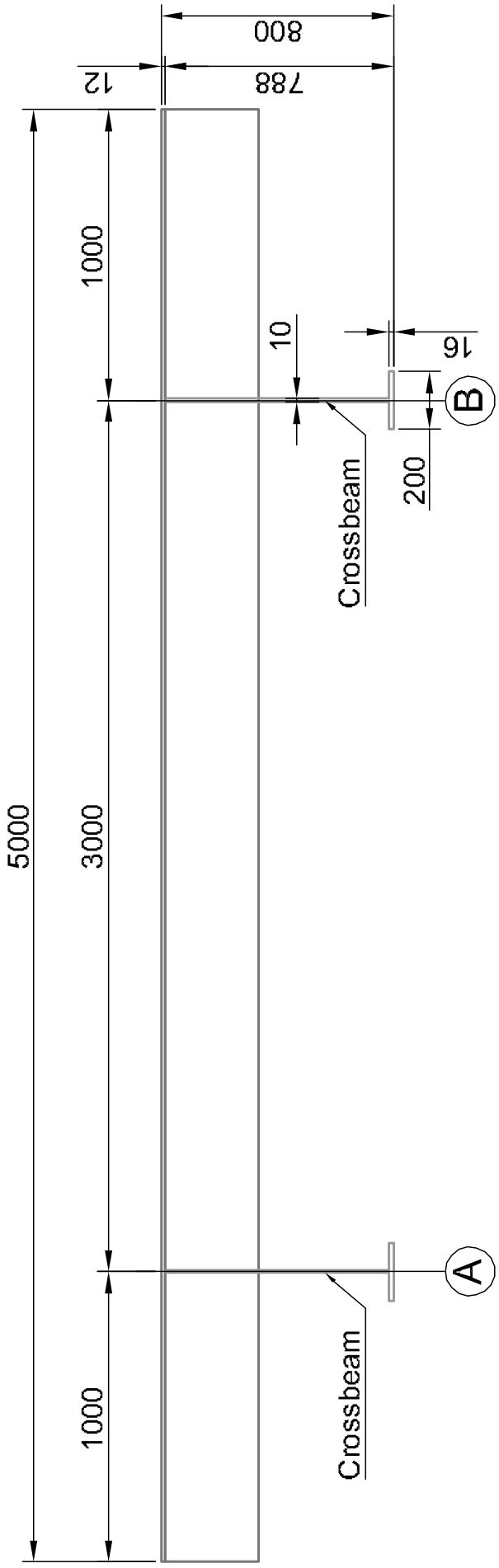

Figure1b

Click here to download Figure fig01b.eps

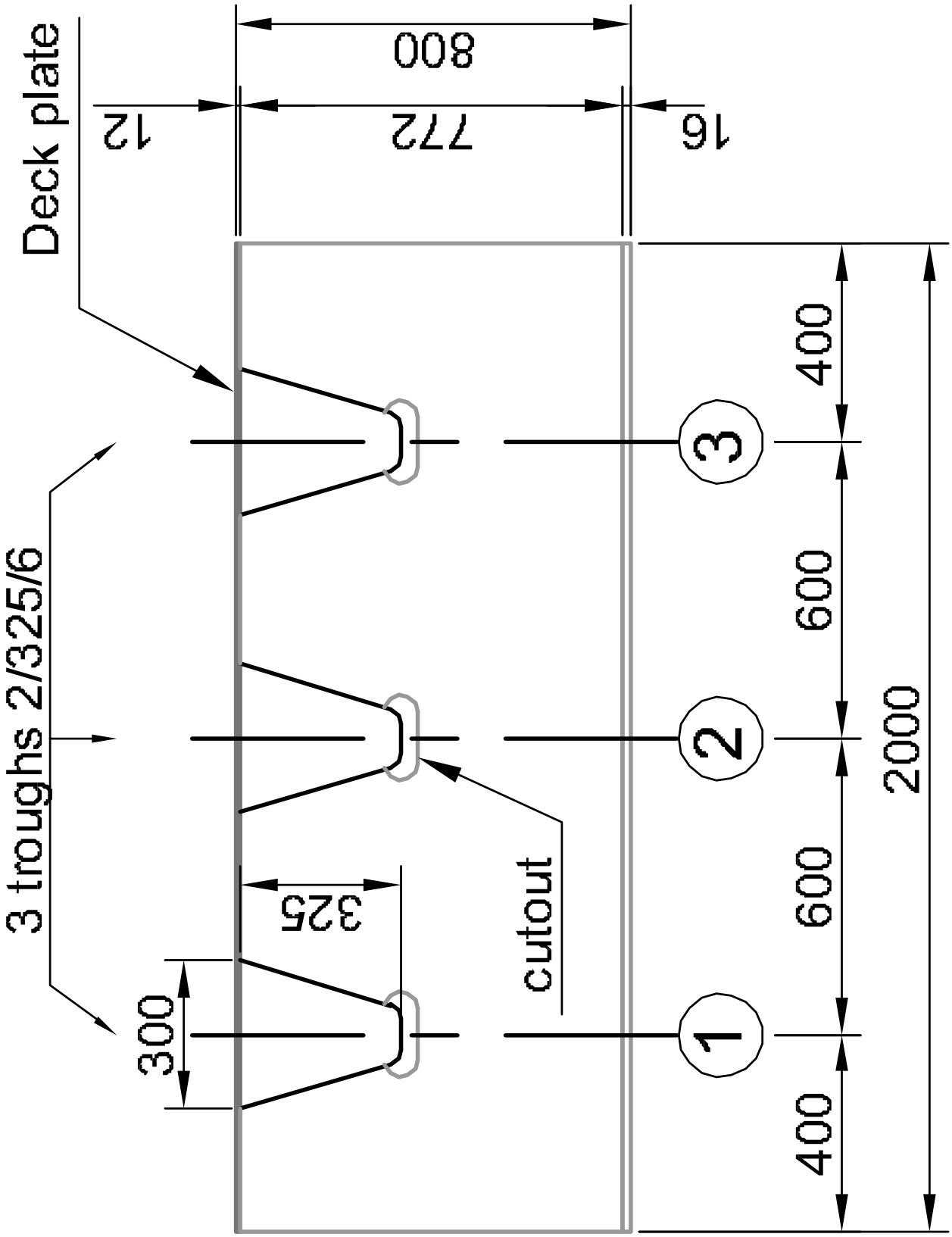

Figure2a

Click here to download Figure fig02a.eps

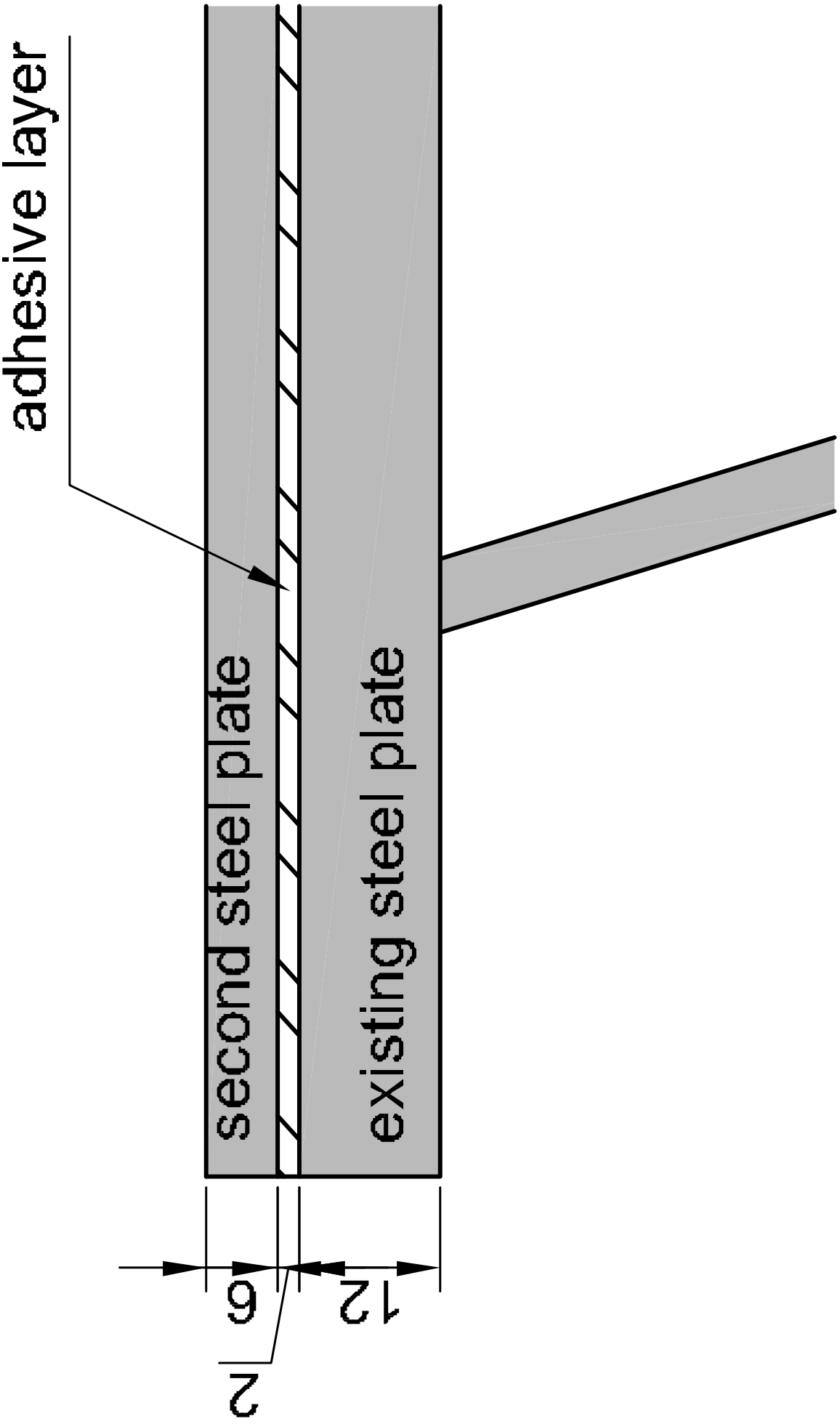

Figure2b

Click here to download Figure fig02b.eps

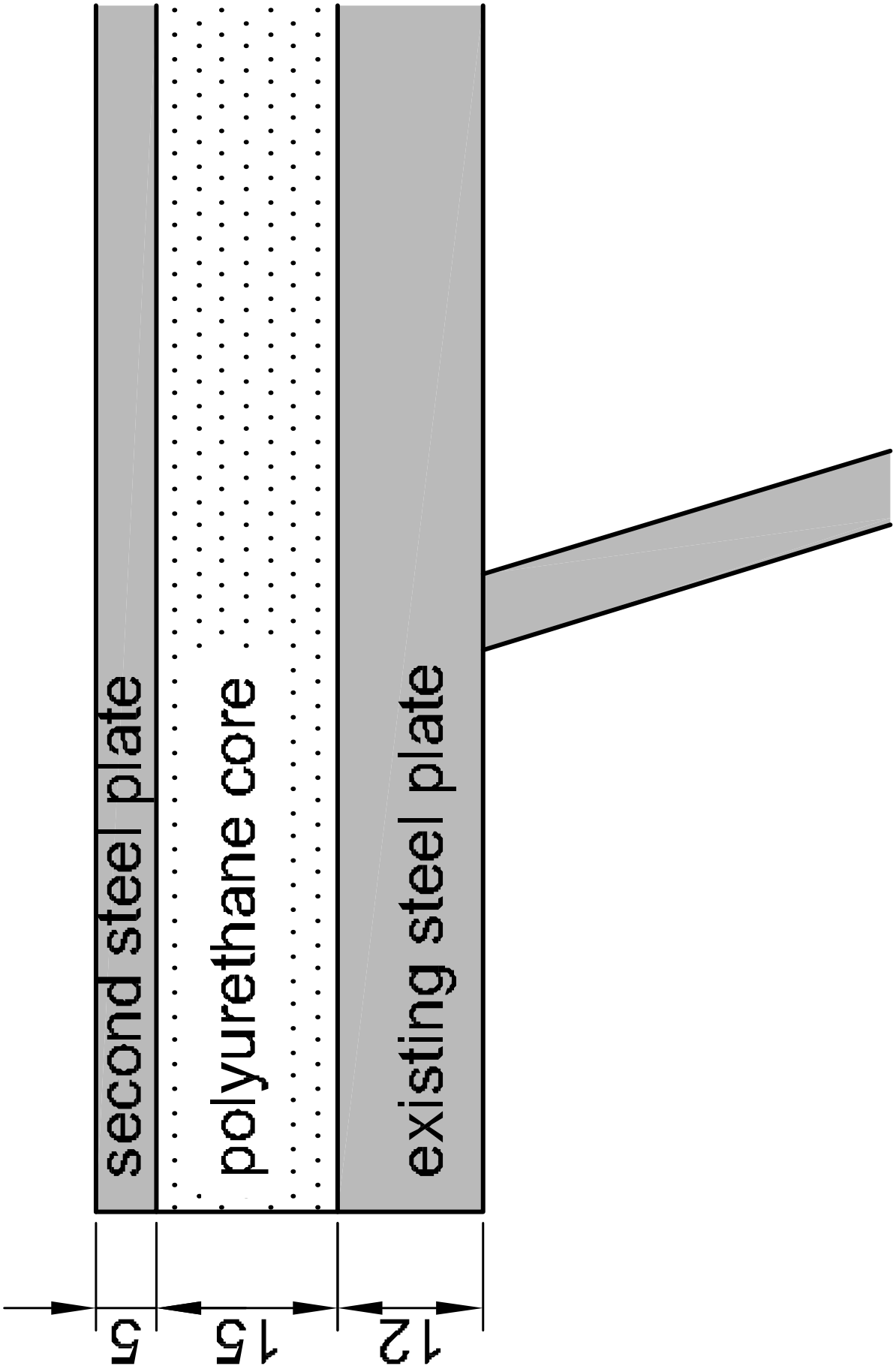

Figure3a

Click here to download Figure fig03a.eps

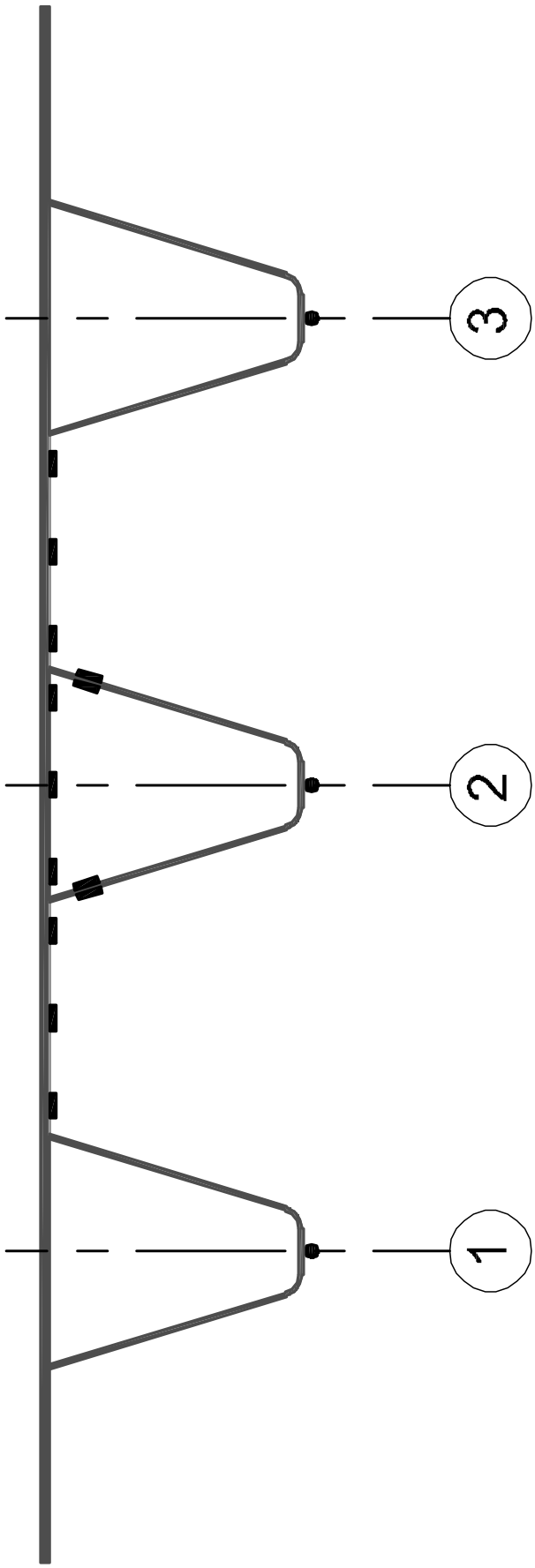

Figure3b

Click here to download Figure fig03b.eps

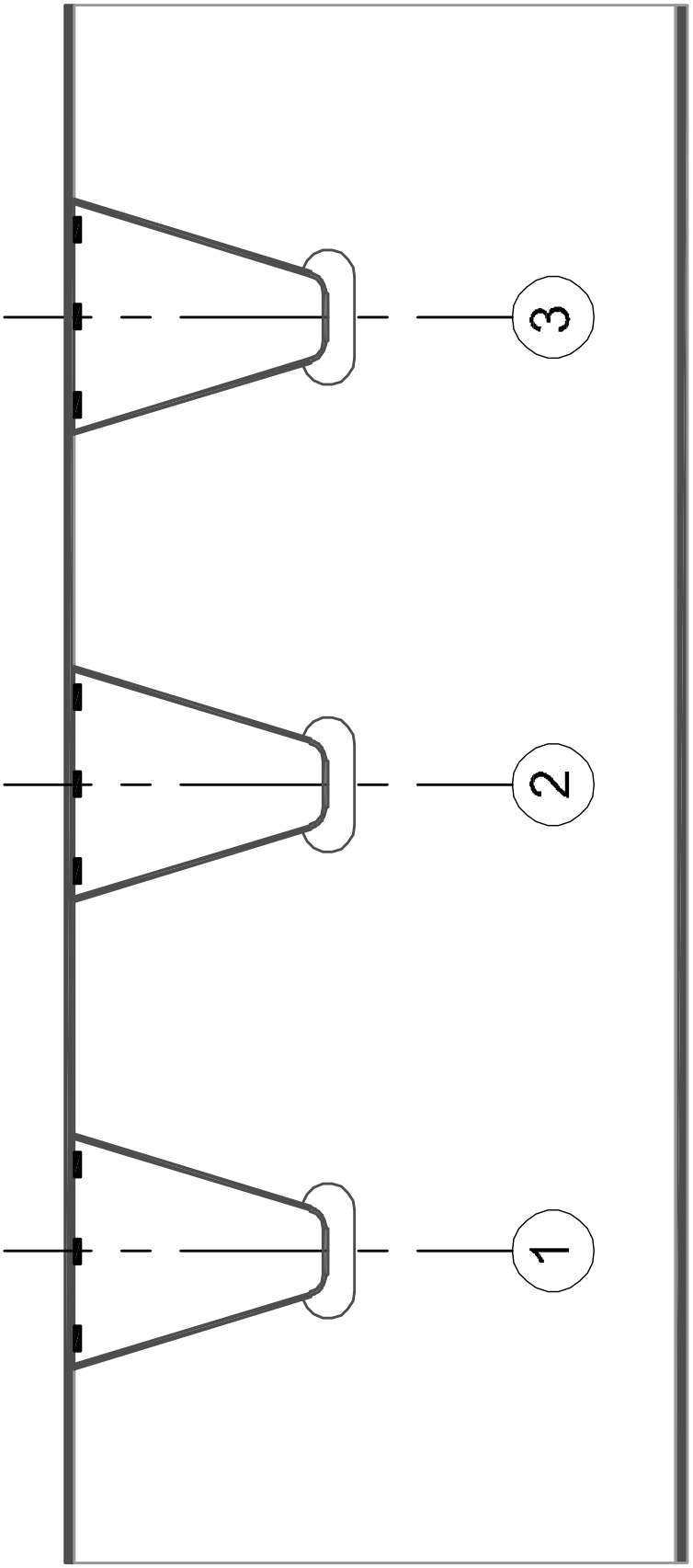

Figure3c

Click here to download Figure fig03c.eps

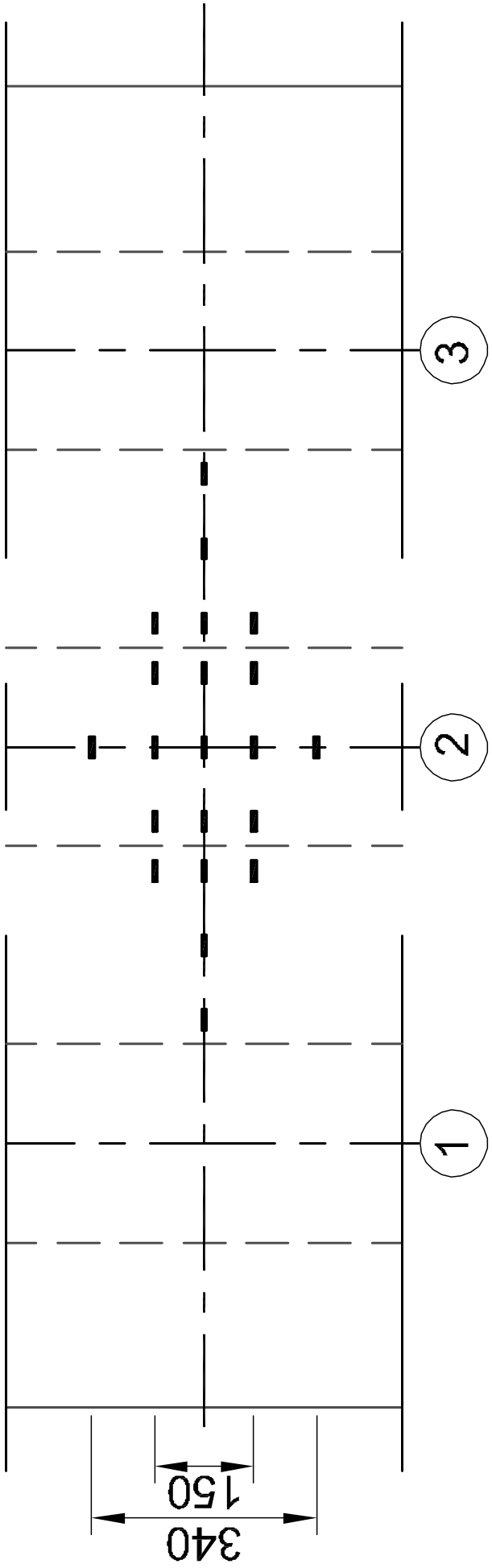

Figure3d

Click here to download Figure fig03d.eps

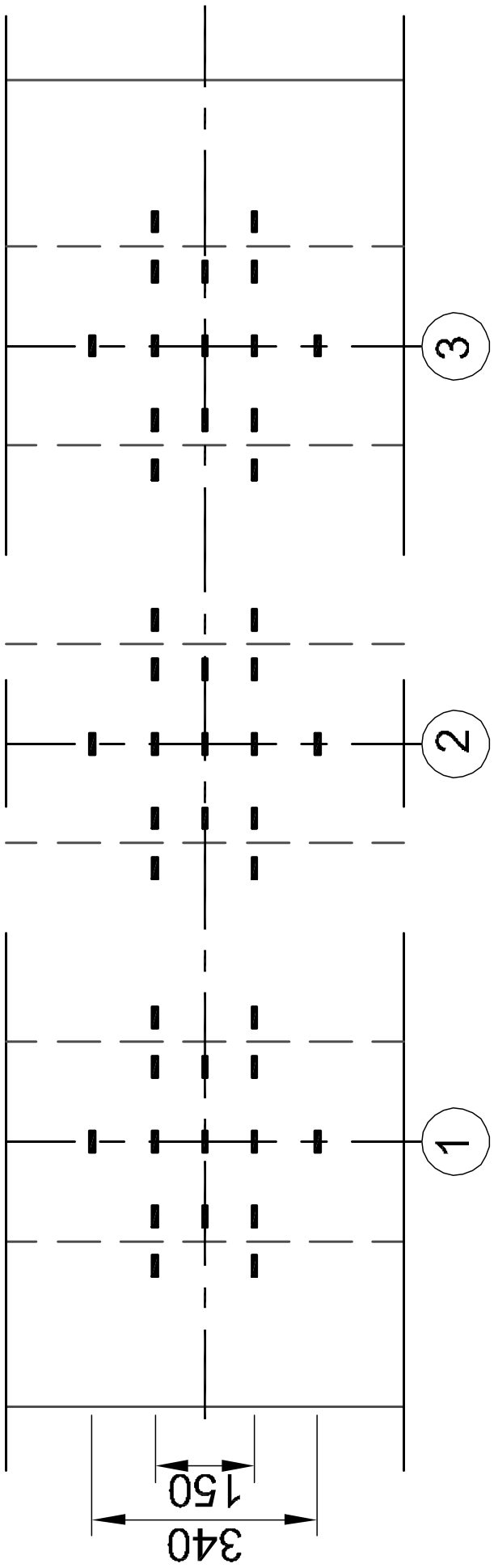

Figure4

Click here to download Figure fig04.eps

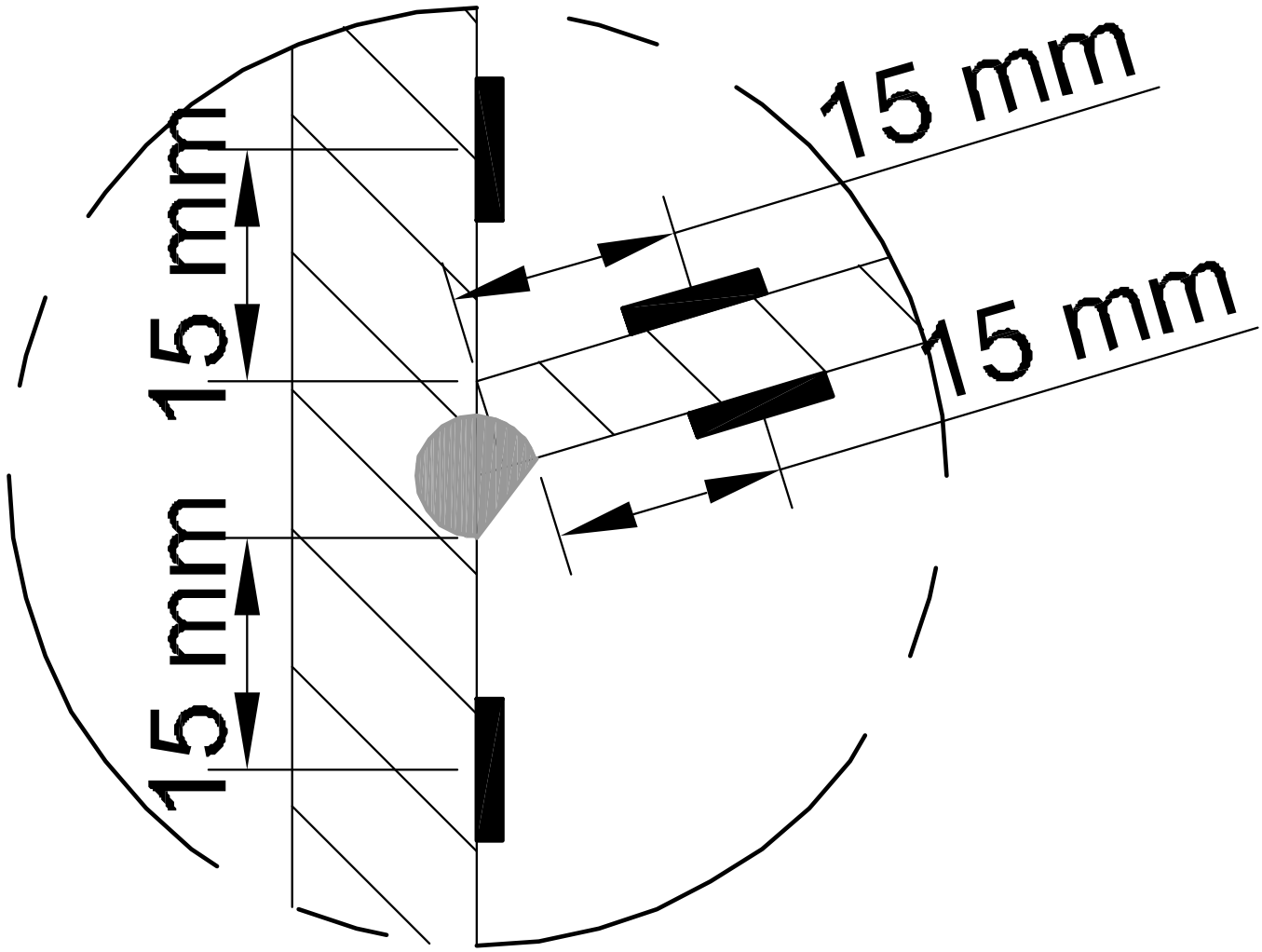

Figure5a

Click here to download Figure fig05a.eps

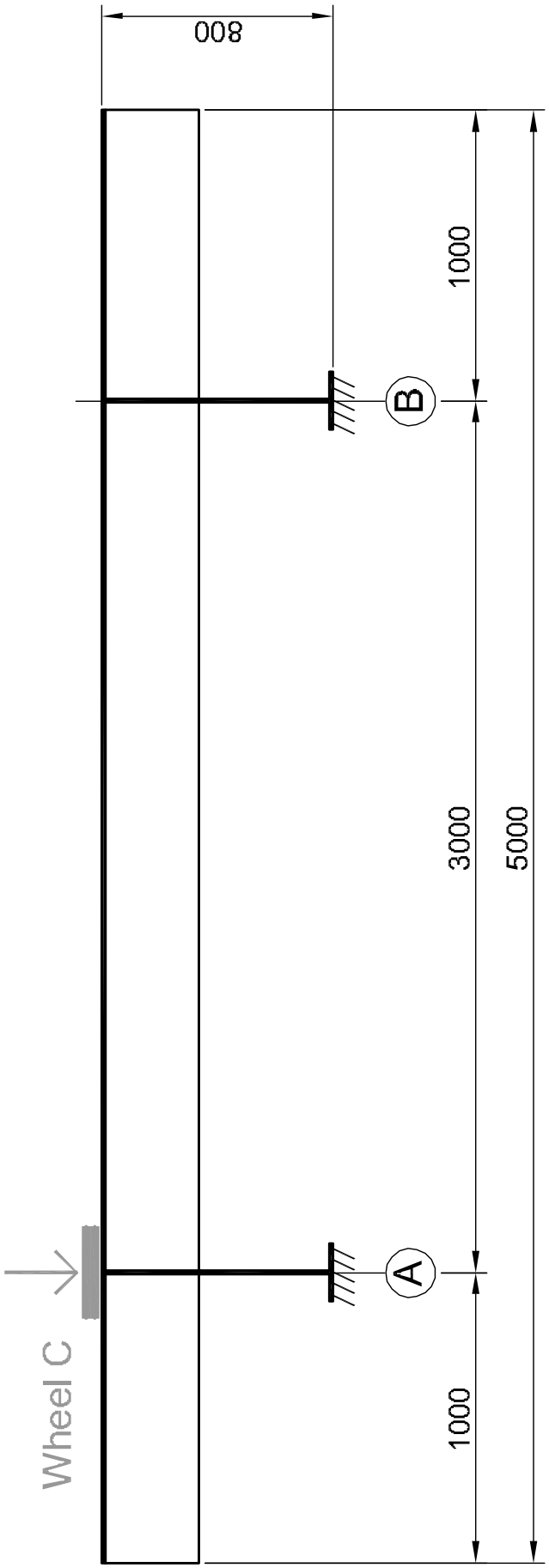

Figure5b

Click here to download Figure fig05b.eps

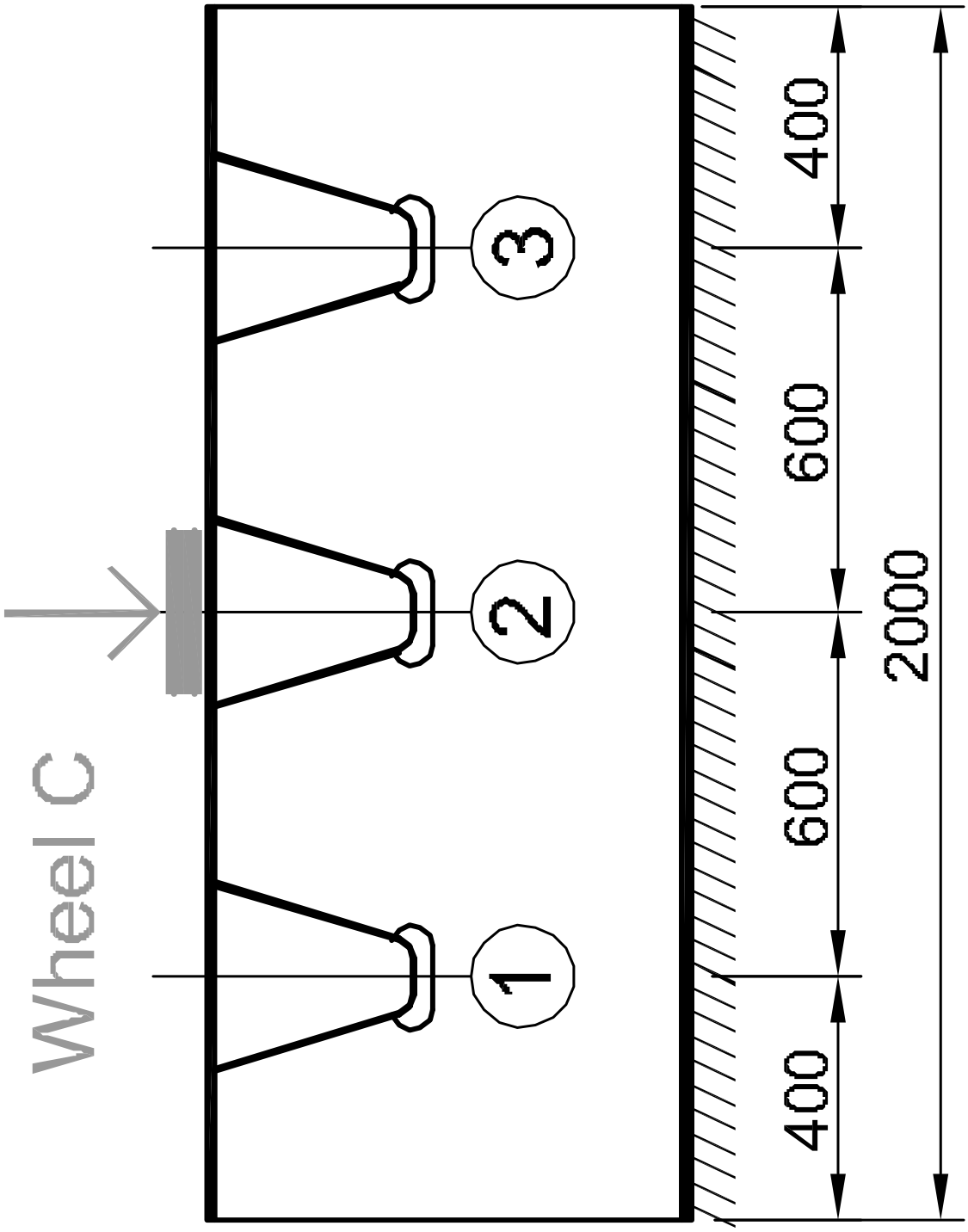

Figure6

Figure7

Click here to download Figure fig07.eps

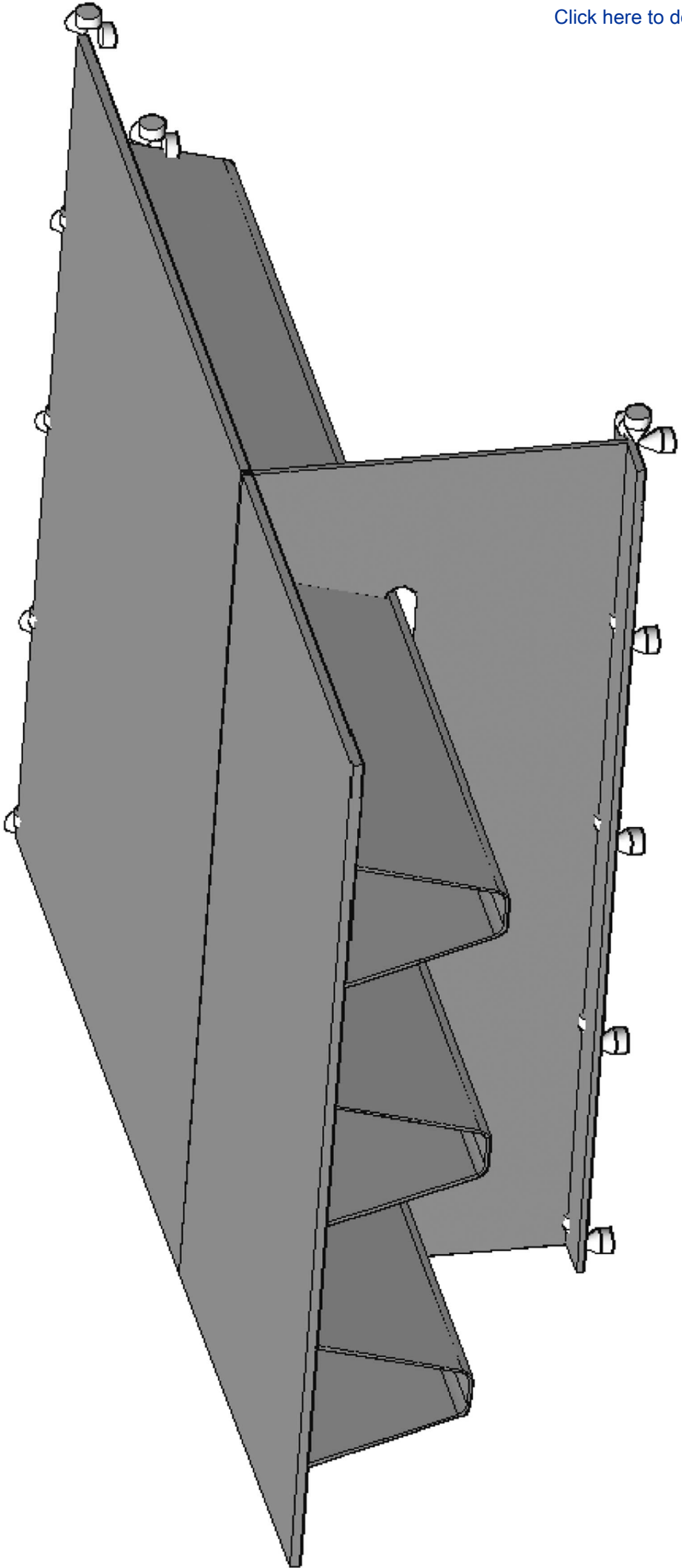

Figure8a

Click here to download Figure fig08a.eps

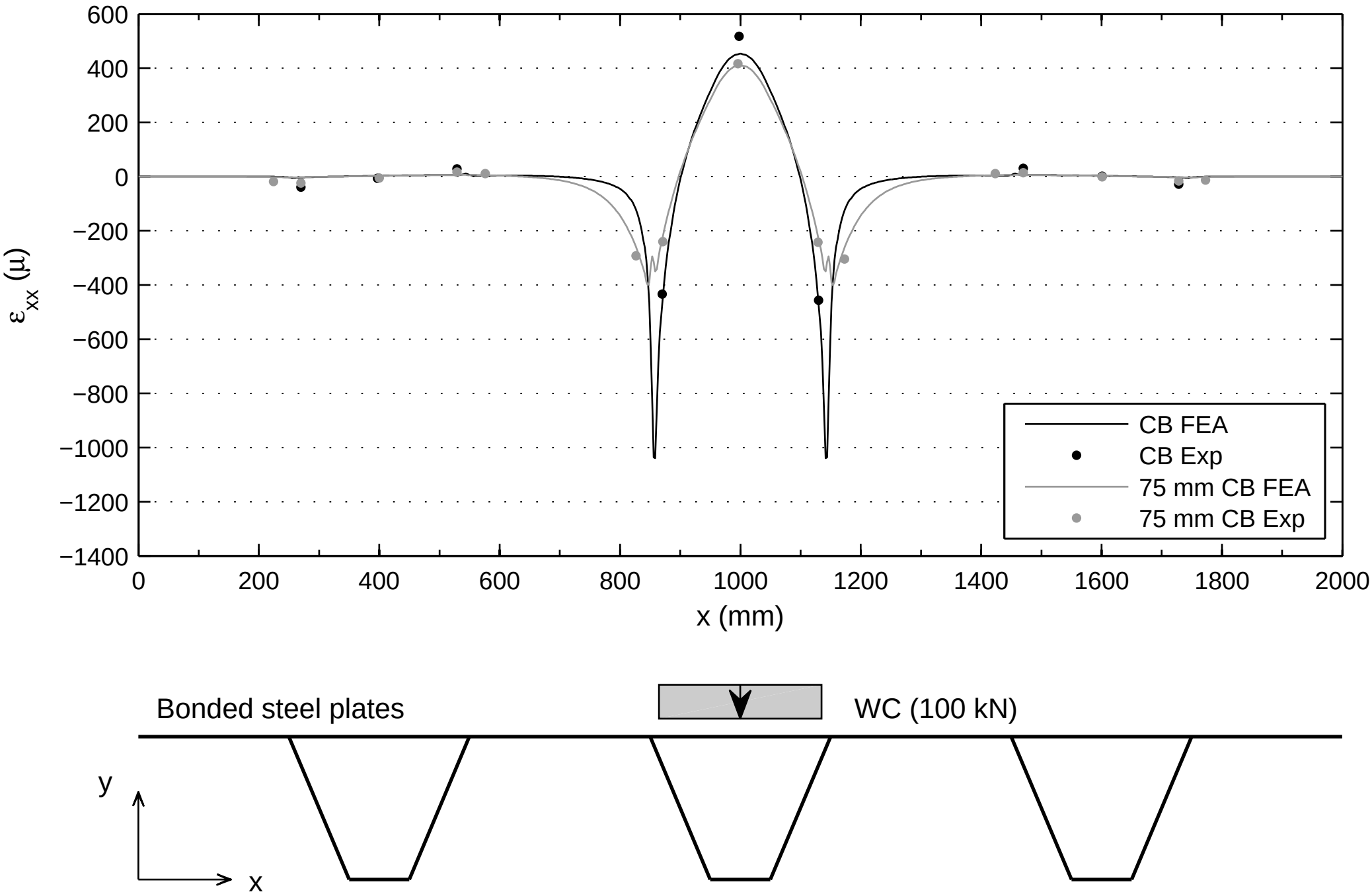

Figure8b

Click here to download Figure fig08b.eps

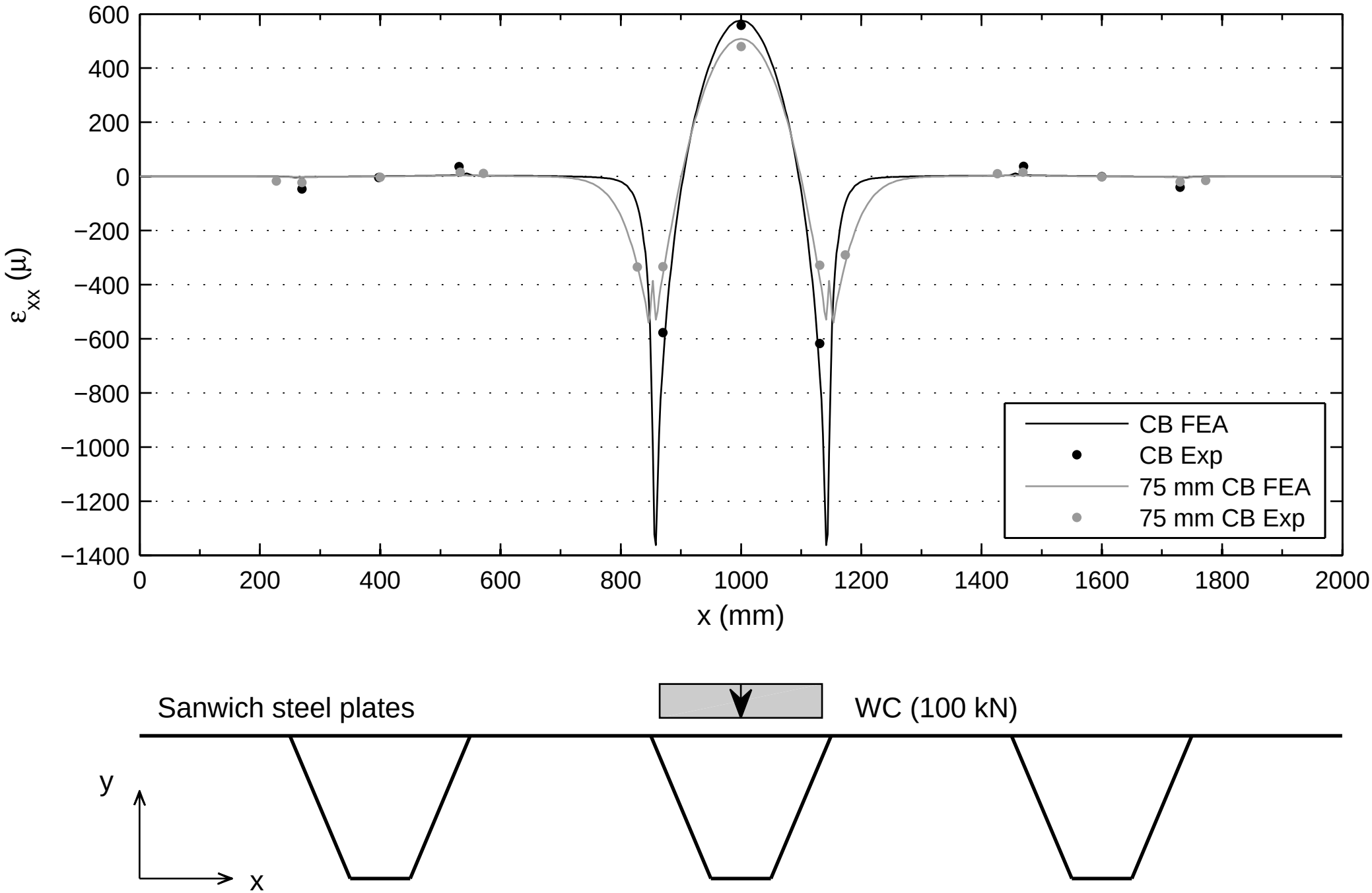

Figure9a

Click here to download Figure fig09a.eps

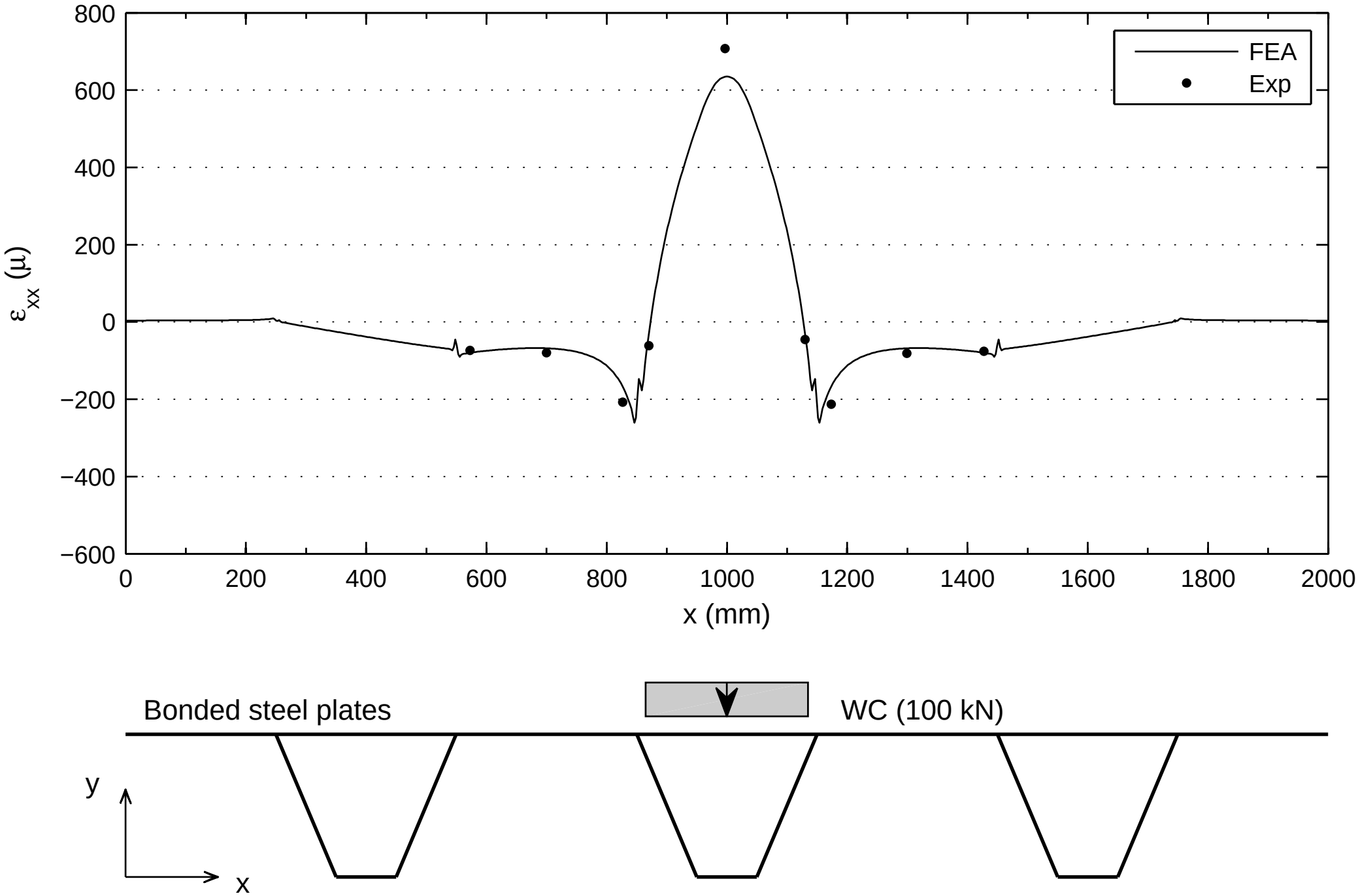

Figure9b

Click here to download Figure fig09b.eps

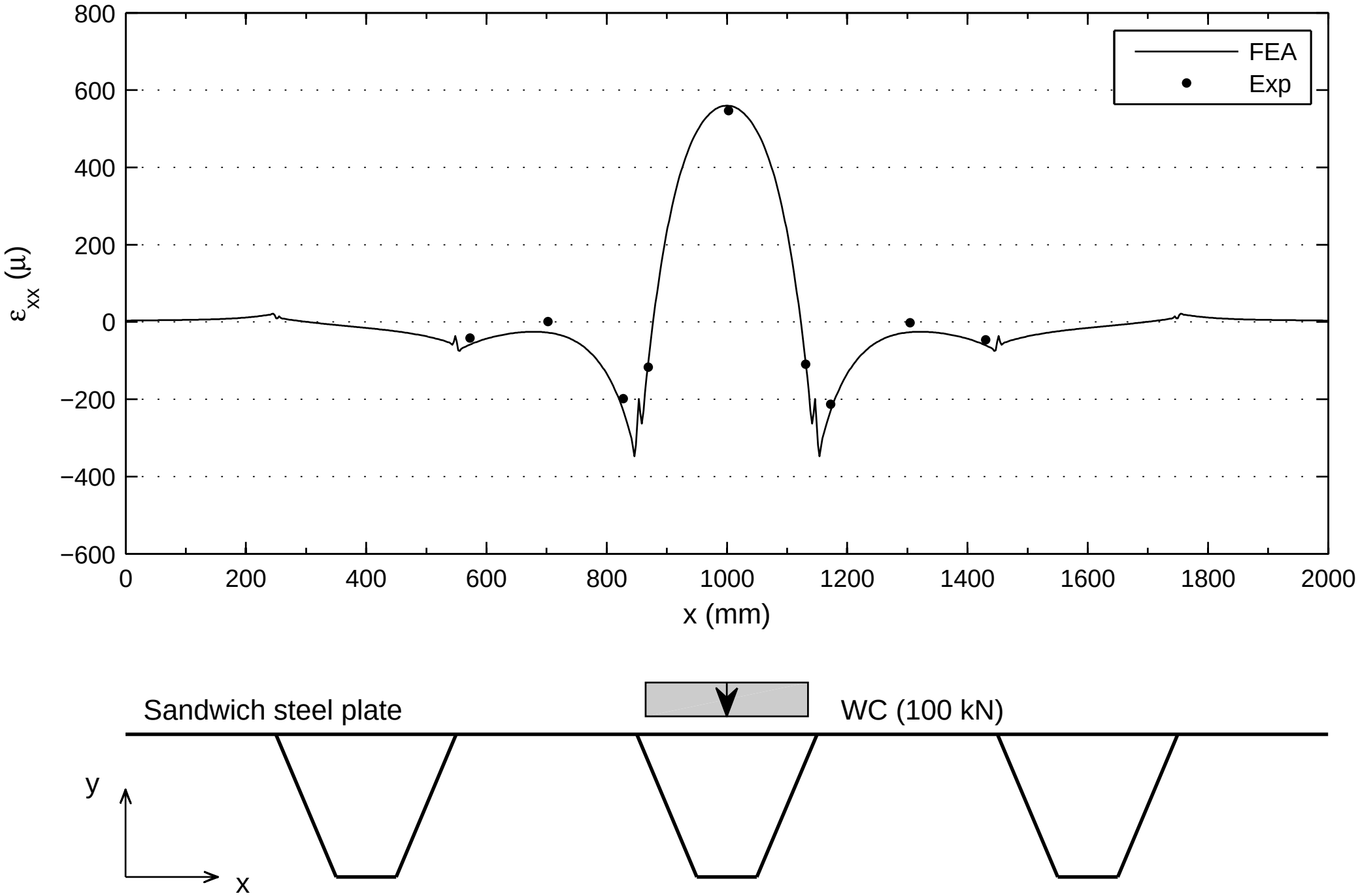

Figure10a

Click here to download Figure fig10a.eps

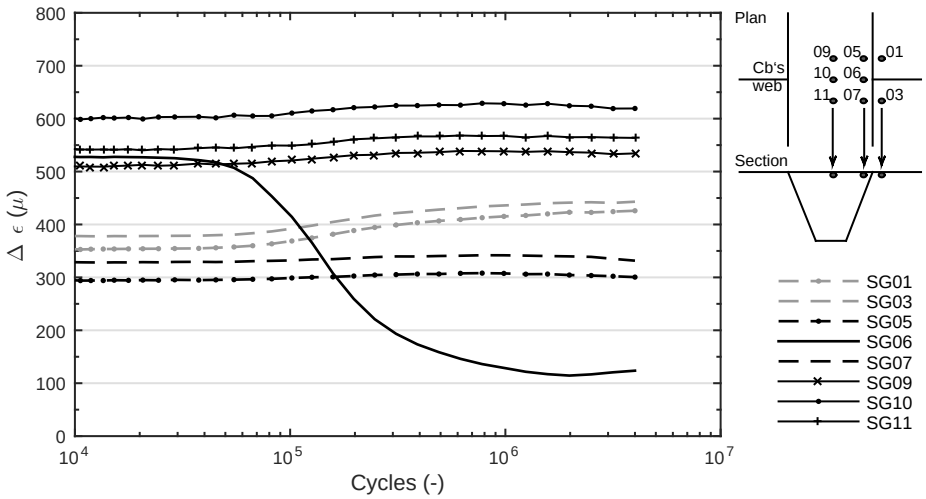

Figure10b

Click here to download Figure fig10b.eps

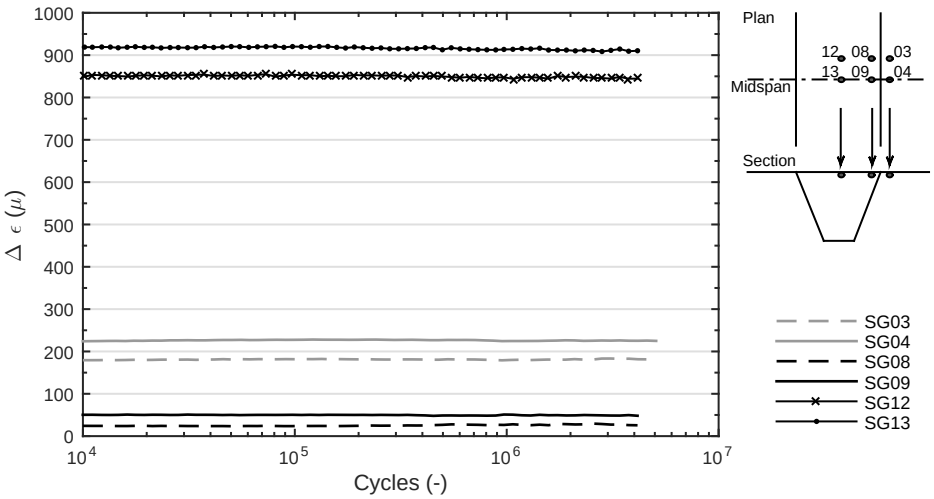

Figure11a

Click here to download Figure fig11a.eps

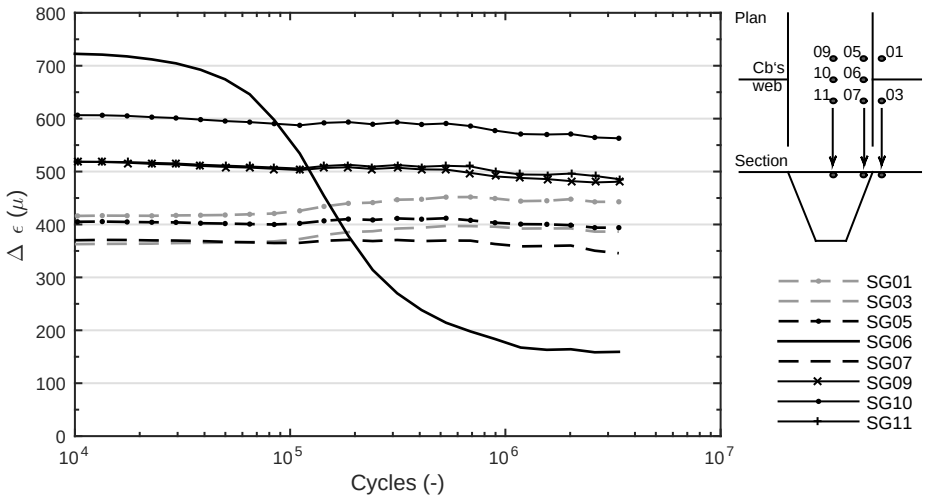

Figure11b

Click here to download Figure fig11b.eps

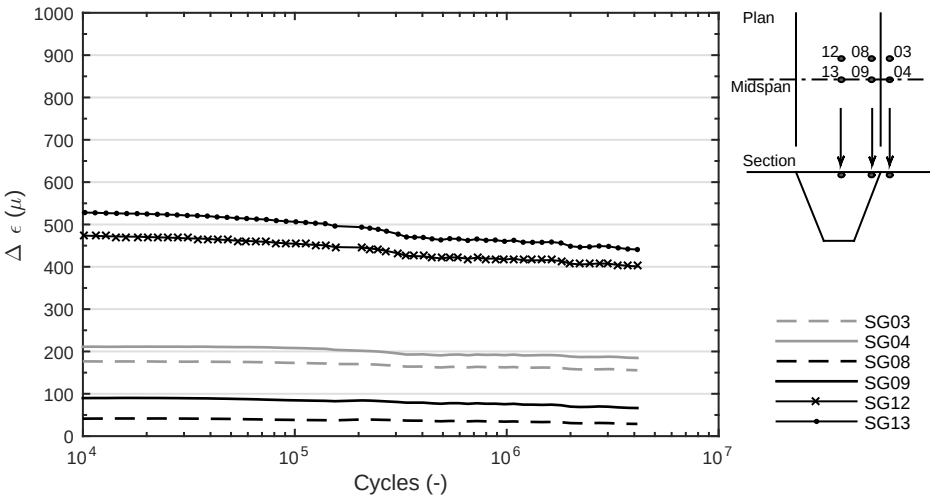

Figure12a

Click here to download Figure fig12a.eps

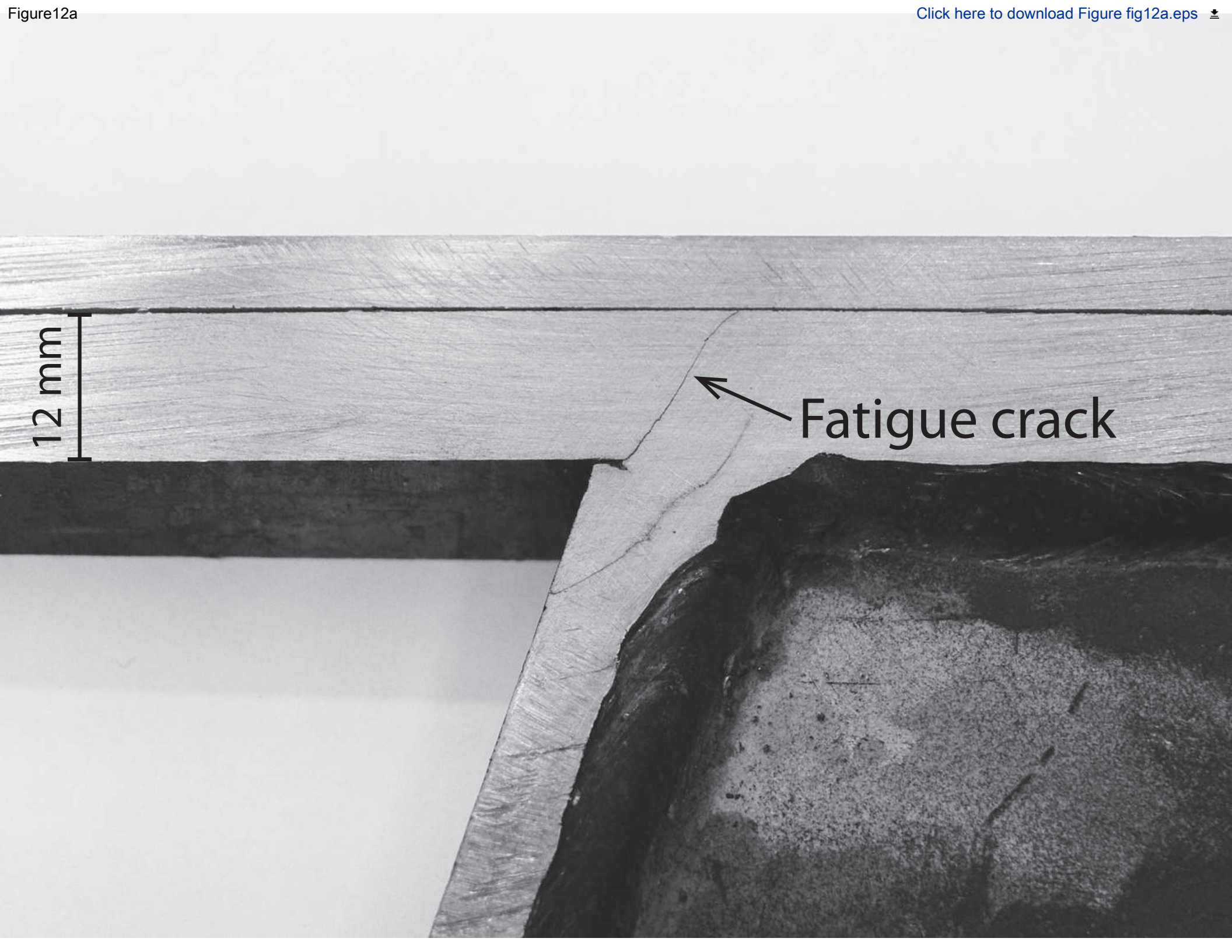

Figure12b

Click here to download Figure fig12b.eps

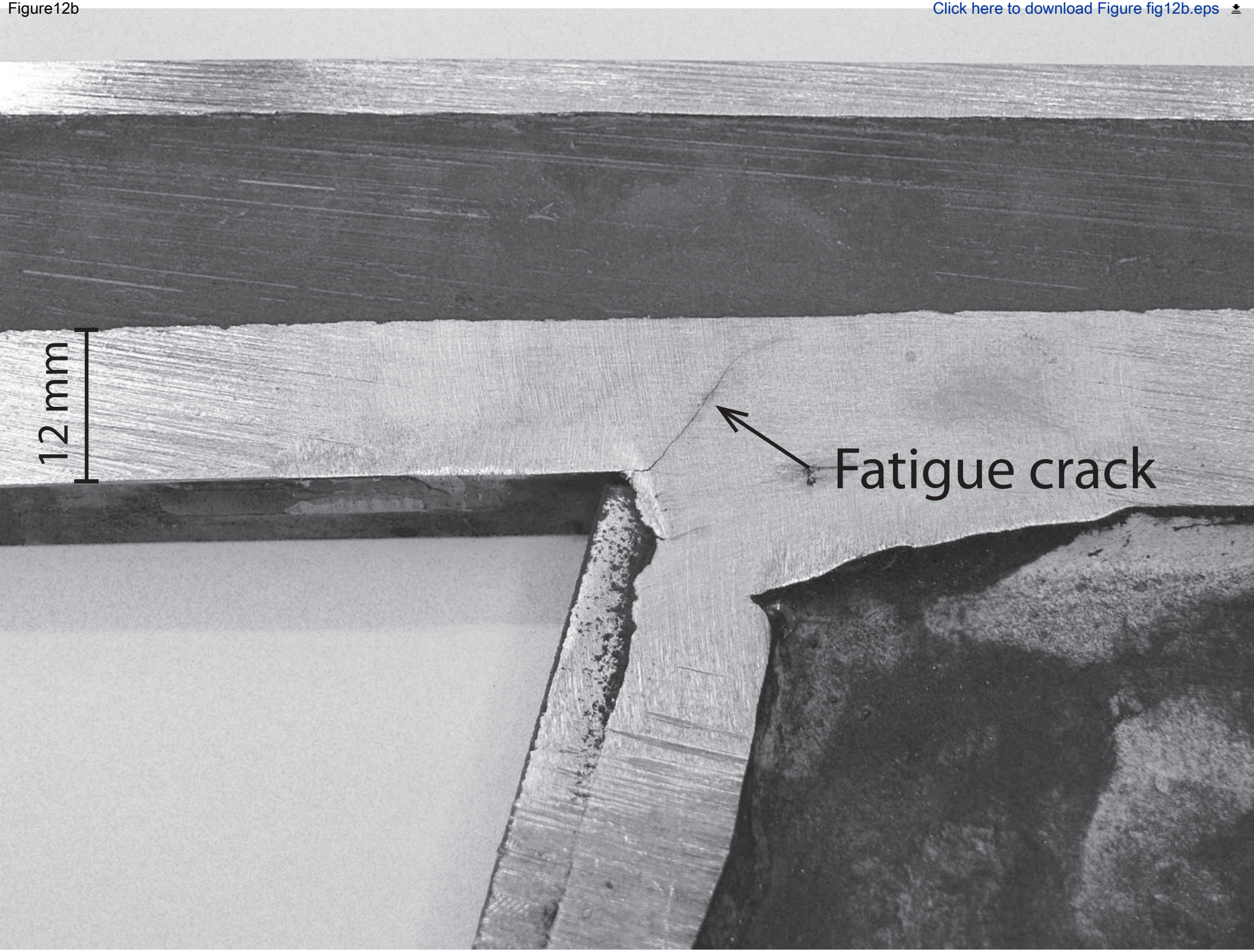

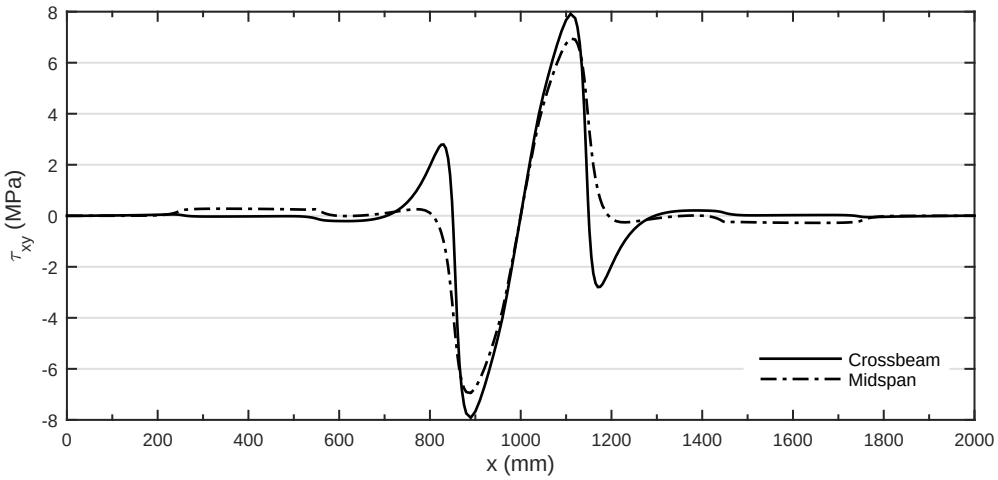

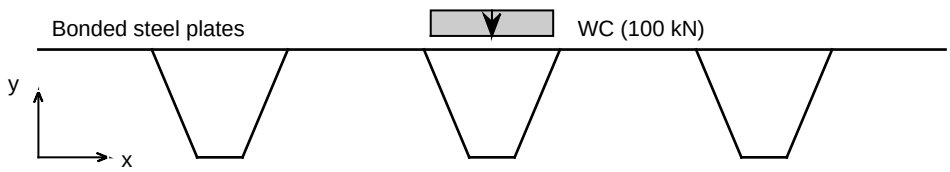

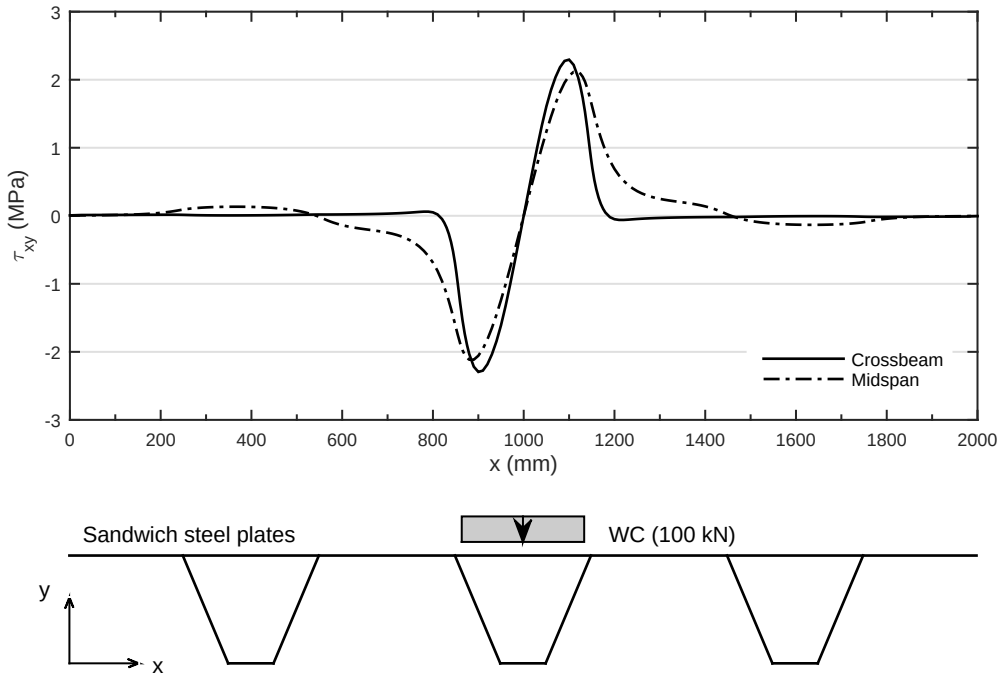

Figure14a

Click here to download Figure fig14a.eps

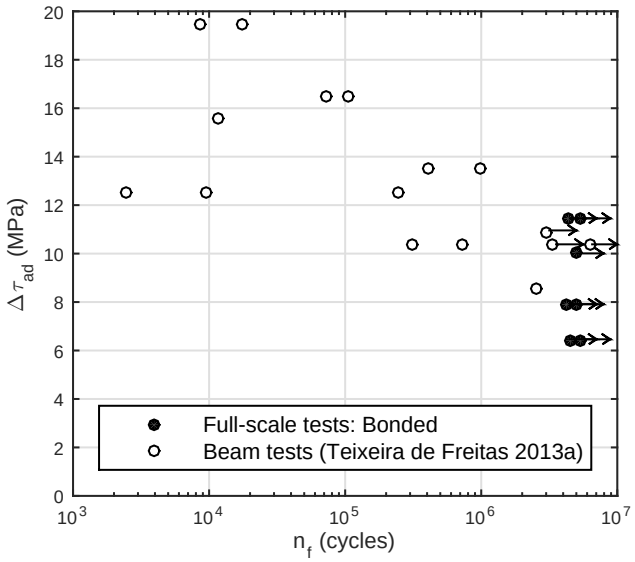

Figure14b

Click here to download Figure fig14b.eps

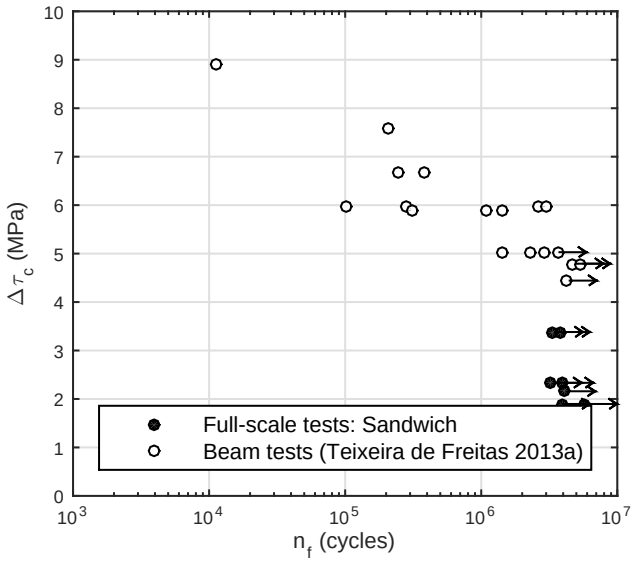

Figure15a

Click here to download Figure fig15a.eps

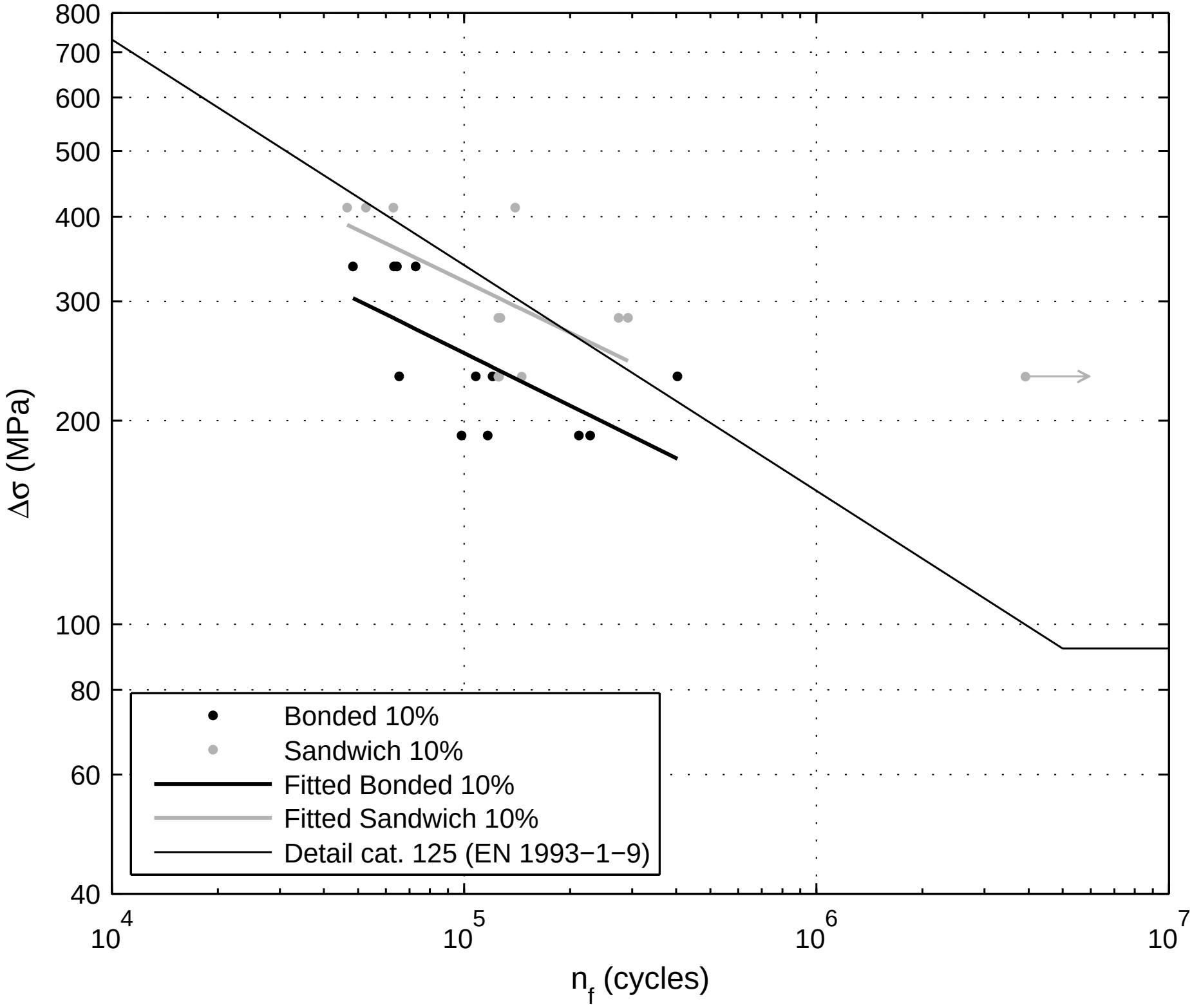

Figure15b

Click here to download Figure fig15b.eps

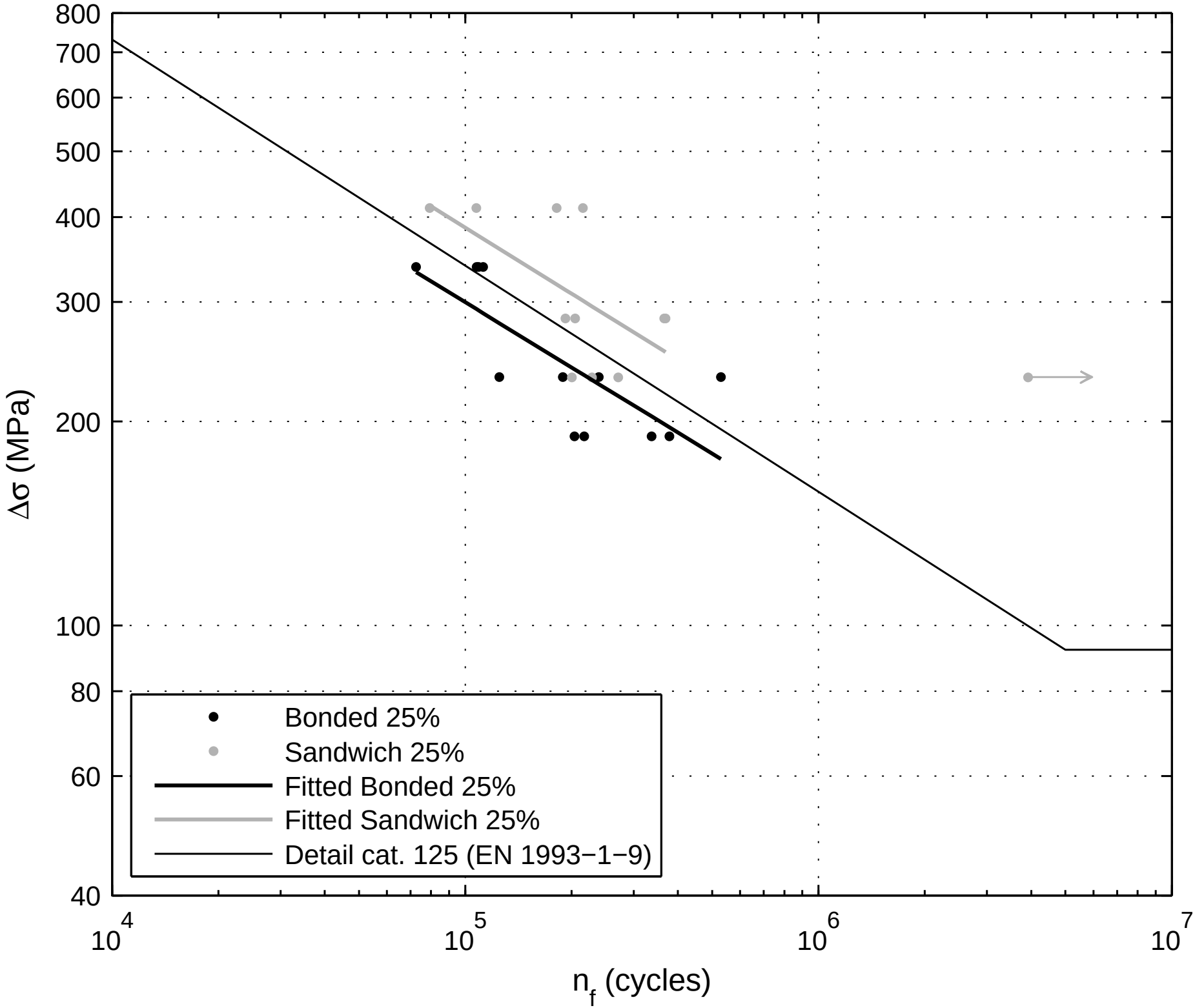

Figure16

Click here to download Figure fig16.eps

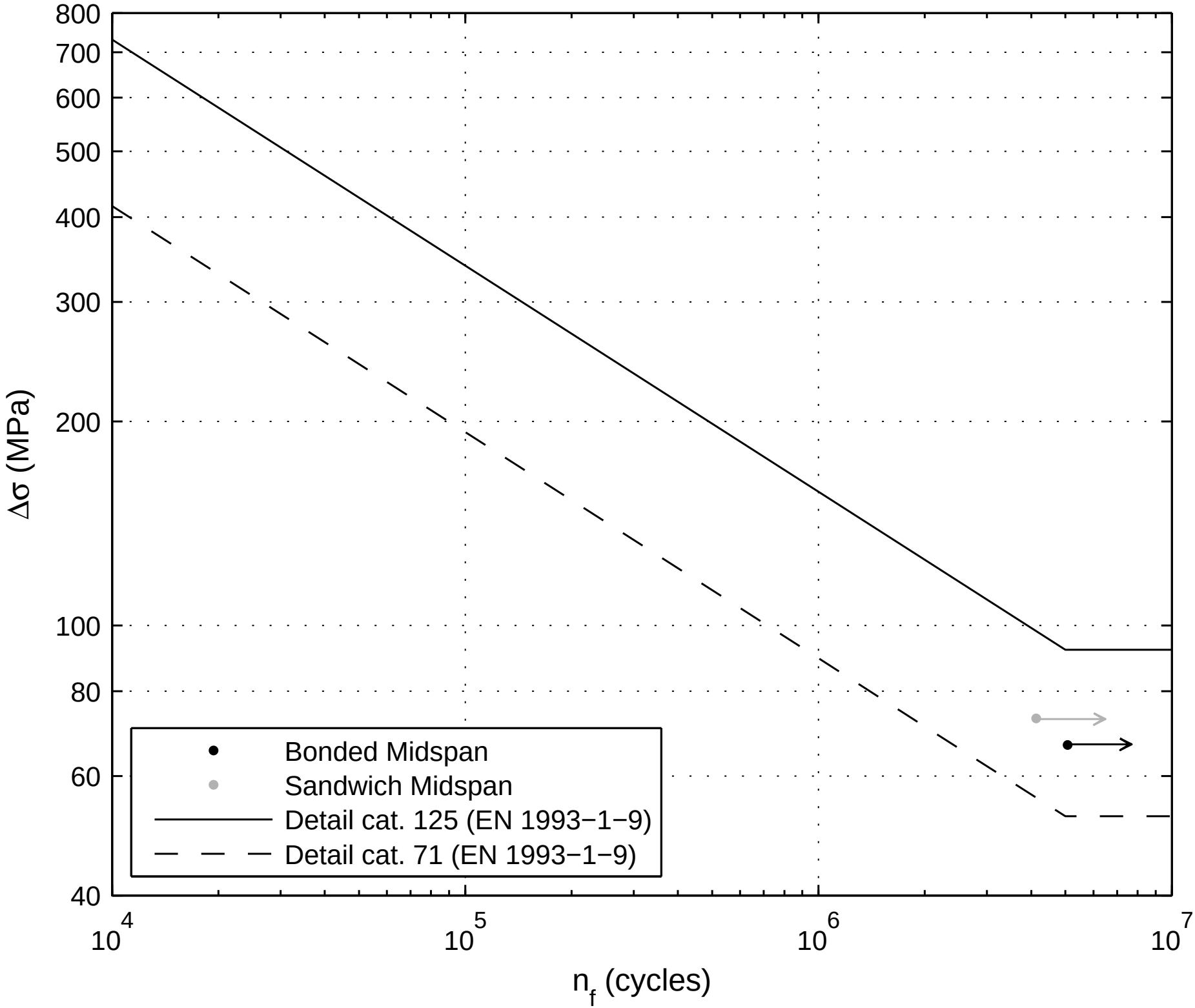

Figure17

Click here to download Figure fig17.eps

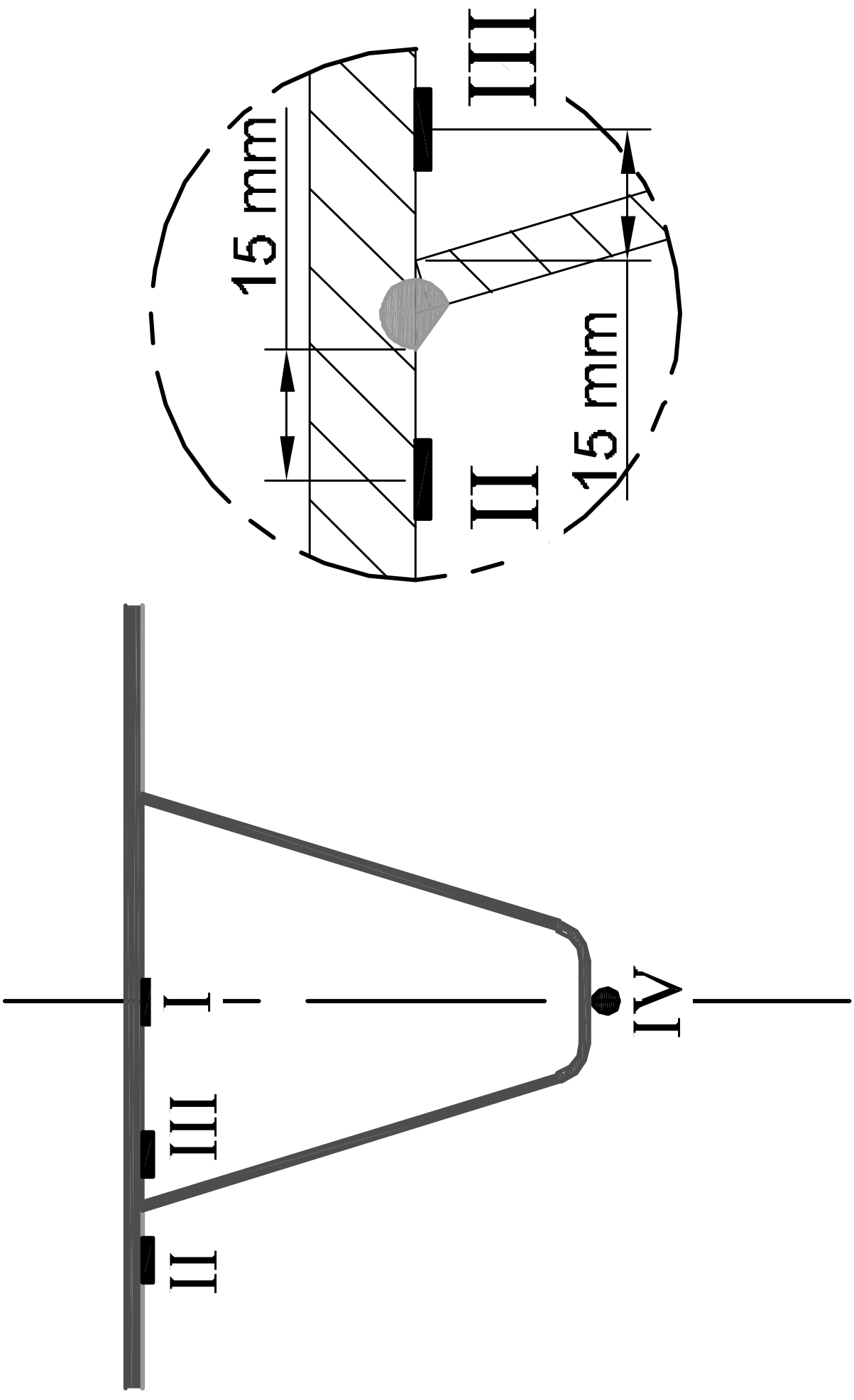

Figure18a

Click here to download Figure fig18a.eps

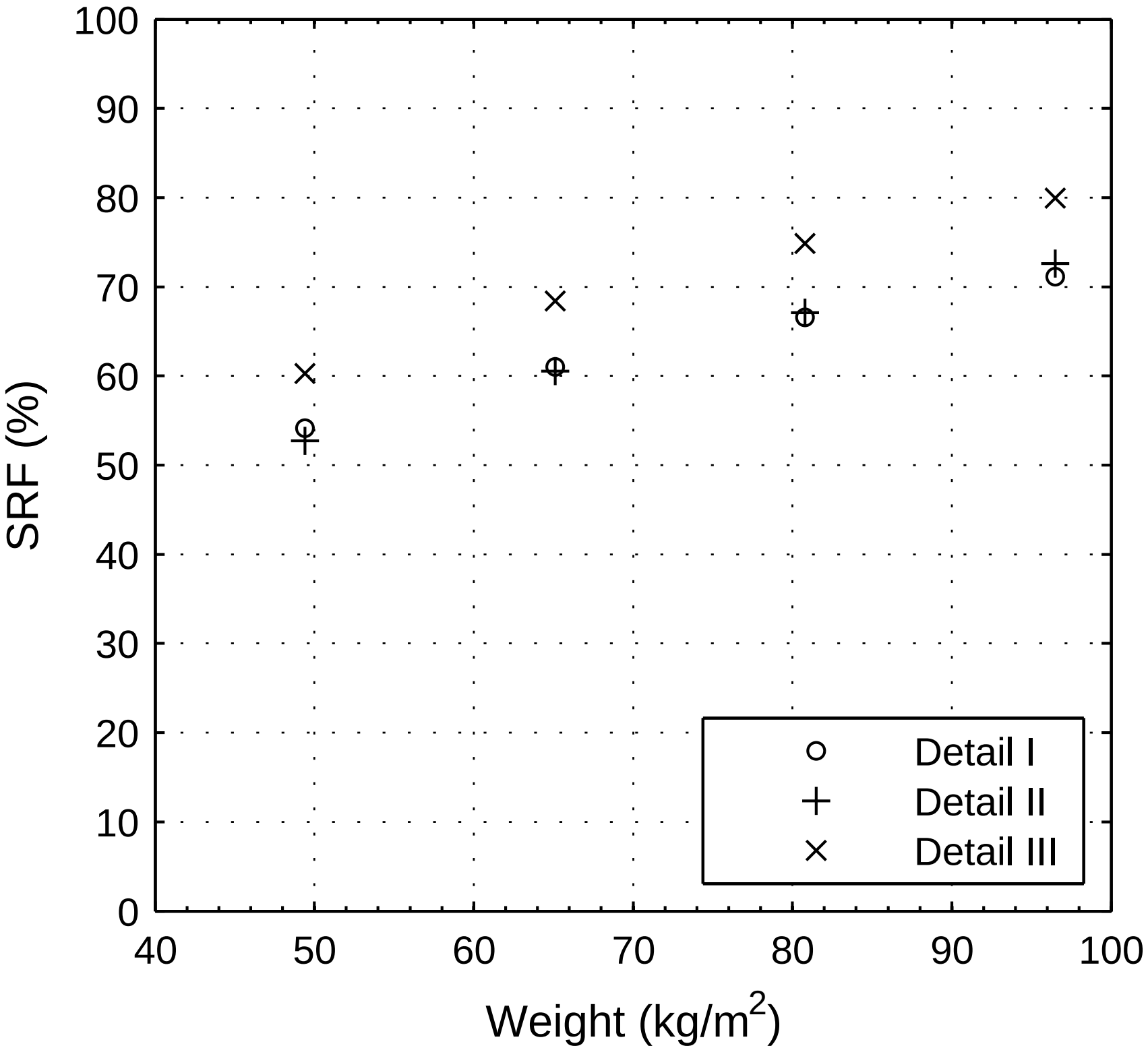

Figure18b

Click here to download Figure fig18b.eps

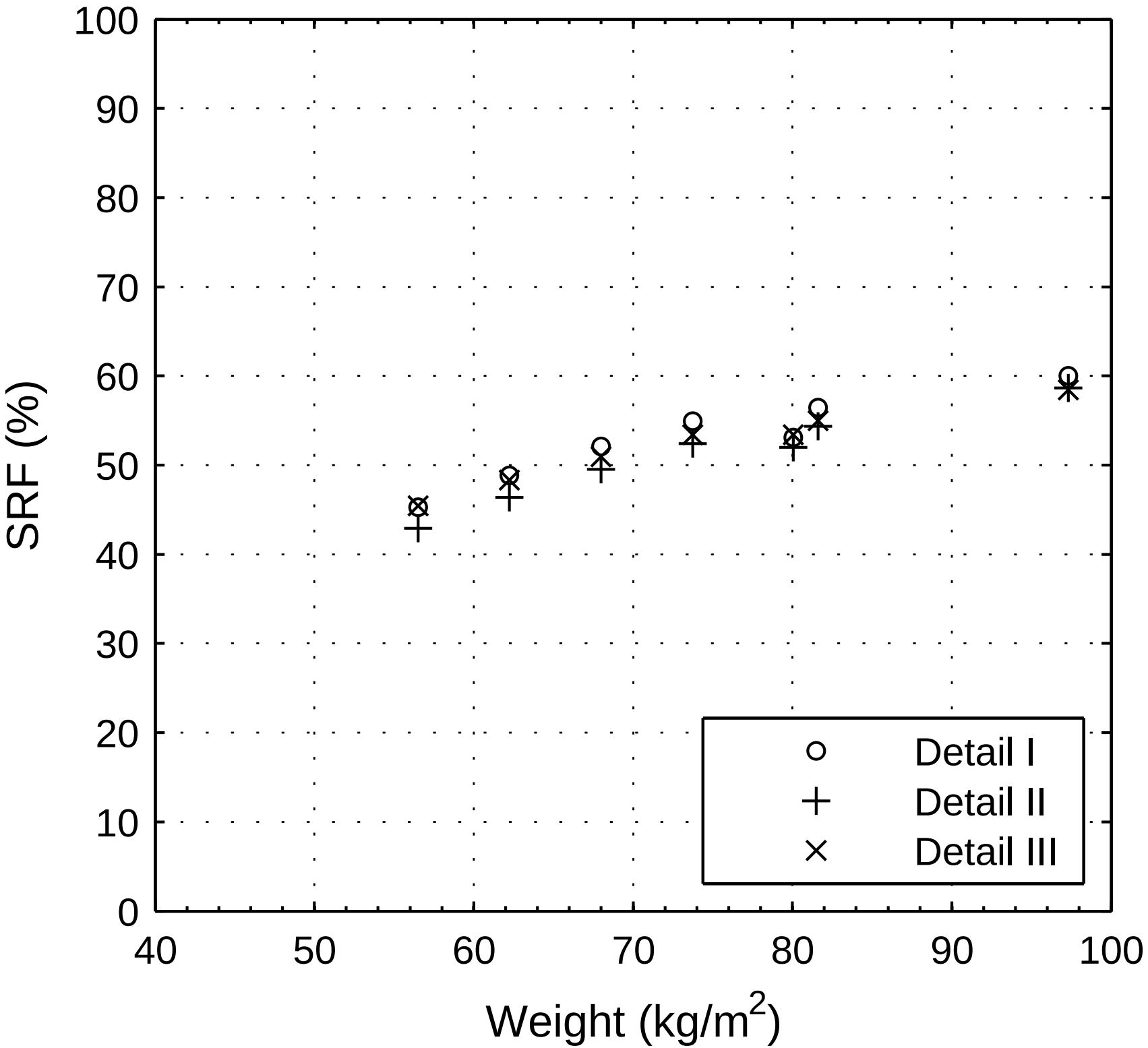

Figure19a

Click here to download Figure fig19a.eps

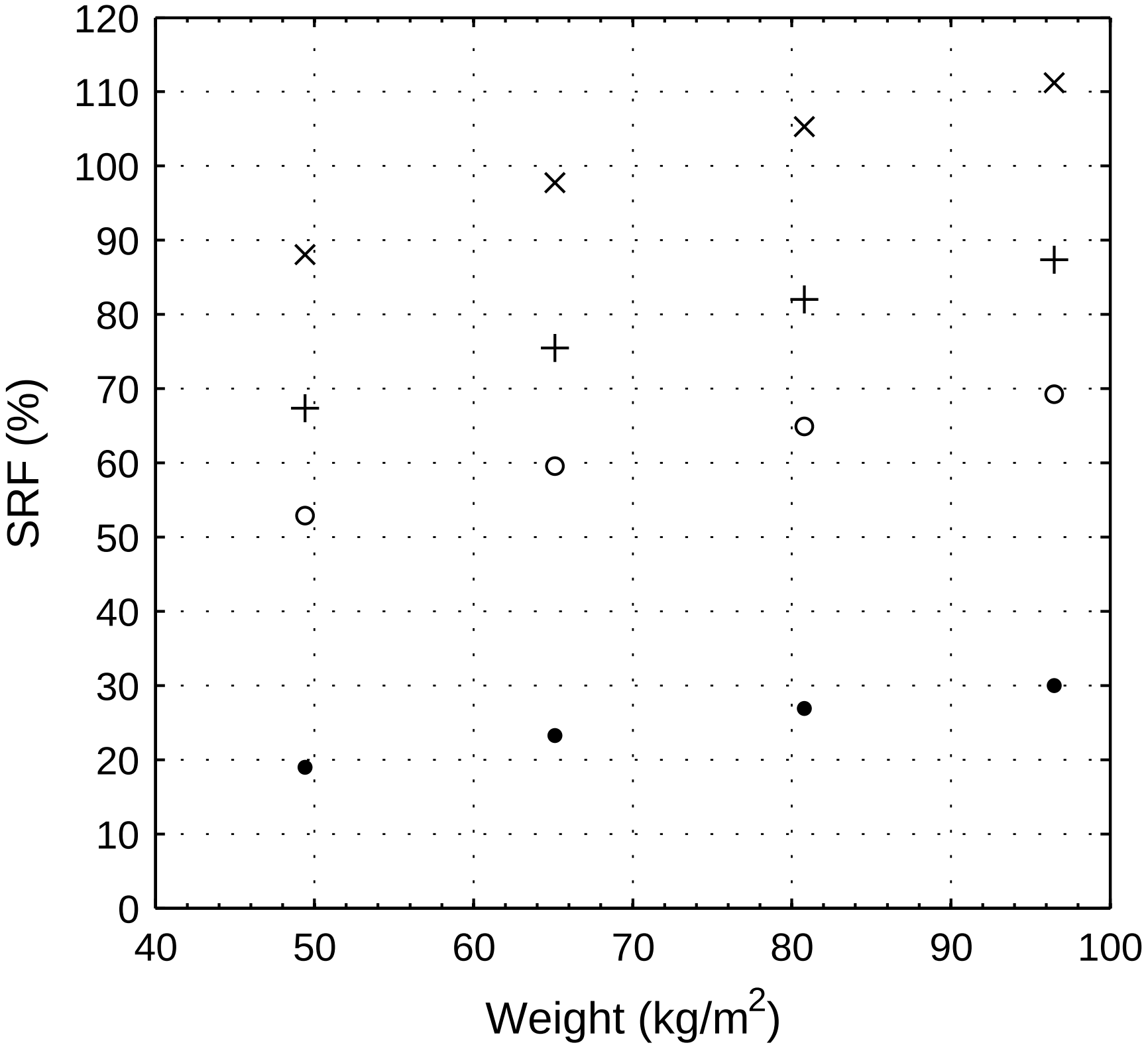

Figure19b

Click here to download Figure fig19b.eps

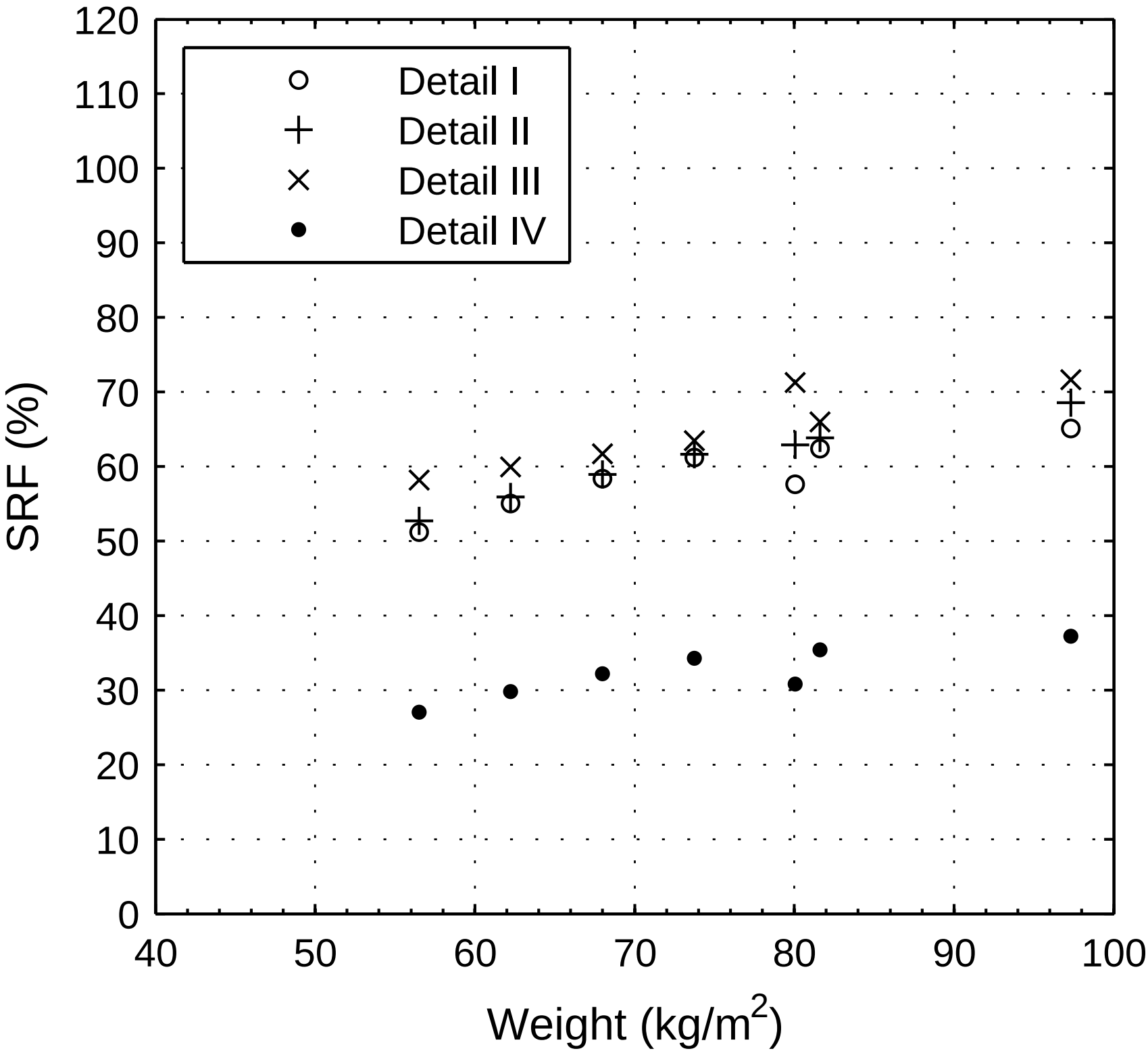

Figure 1- Geometry of the deck specimens (dimensions in mm). (a) Longitudinal cross section; (b) Transverse cross section

Figure 2 – Retrofitting systems (dimensions in mm). a) Bonded system; b) Sandwich system

Figure 3 – Strain gauges location (dimensions in mm). (a) Midspan; (b) Crossbeam; (c) Top view of the midspan; (d) Top view of the crossbeam

Figure 4 – Position of the strain gauges close to the deck-to-stiffener weld.

Figure 5- Example of a fatigue test performed at the crossbeam location (crossbeam A, trough 2). (a) Longitudinal view; (b) Crossbeam A cross-section

Figure 6 – Experimental test set-up.

Figure 7 - Three-dimensional finite element model overview (Teixeira de Freitas 2013b).

Figure 8 - Transverse strains ε_{xx} at the crossbeam (CB) and 75 mm from the crossbeam (75 mm CB) on the bottom side of the deck plate recorded during testing (Exp) and predicted by the FEA (Teixeira de Freitas 2013b). a) bonded system, b) sandwich system

Figure 9 - Transverse strains εxx at midspan on the bottom side of the deck plate recorded during testing (Exp) and predicted by the FEA (Teixeira de Freitas 2013b).

a) bonded system, b) sandwich system

Figure 10 – Strain ranges measured during fatigue tests of the bonded steel plates reinforced deck specimen.

(a) Example of strains at a crossbeam fatigue test: P_{max} = 160 kN (ΔP = 144 kN).

(b) Strains at the midspan between crossbeams: P_{max} = 160 kN (ΔP = 144 kN).

Figure 11 – Strain ranges measured during fatigue tests of the sandwich steel plates reinforced deck specimen

(a) Example of strains at a crossbeam fatigue test: P_{max} = 160 kN (ΔP = 144 kN)

(b) Strains at the midspan between crossbeams fatigue test: P_{max} = 110 kN (ΔP = 99 kN).

Figure 12 – Fatigue cracks in deck-plate-to-stiffener welds at the crossbeam location (Pmax=160 kN, ΔP=144 kN). (a) Bonded steel plates reinforced deck. (b) Sandwich steel plates reinforced deck.

Figure 13 – Shear stress distribution τ_{xy} of the reinforced decks loaded at the middle trough by wheel type C at the crossbeam cross section or at midspan between crossbeams (100 kN).

(a) Shear stress in the adhesive layer (mid-thickness) of the bonded steel plates system.

(b) Shear stress at the steel-core interface (max between the two interfaces) of the sandwich steel plate system.

Figure 14– Comparison of the SN diagrams of the reinforcements in the full-scale fatigue tests

and in the bending fatigue tests. (a) bonded system, (b) sandwich system

Figure 15 – Comparison between the SN fatigue results of the welds at the crossbeam cross sections and the detail categories defined in EN 1993-1-9 (2005). (a) 10% strain fall criterion; (b) 25% strain fall criterion.

Figure 16 – Comparison between the SN fatigue results of the welds at midspan between crossbeams and the detail categories defined in EN 1993-1-9 (2005).

Figure 17 – Deck detail location (I to III transverse stresses and IV longitudinal stresses).

Figure 18 – Stress reduction factor (SRF) at the cross beam location for different reinforcement weight scenarios. (a) bonded system, (b) sandwich system.

Figure 19 – Stress reduction factor (SRF) at midspan between crossbeams for different reinforcement weight scenarios. (a) bonded system, (b) sandwich system.